LUND UNIVERSITY

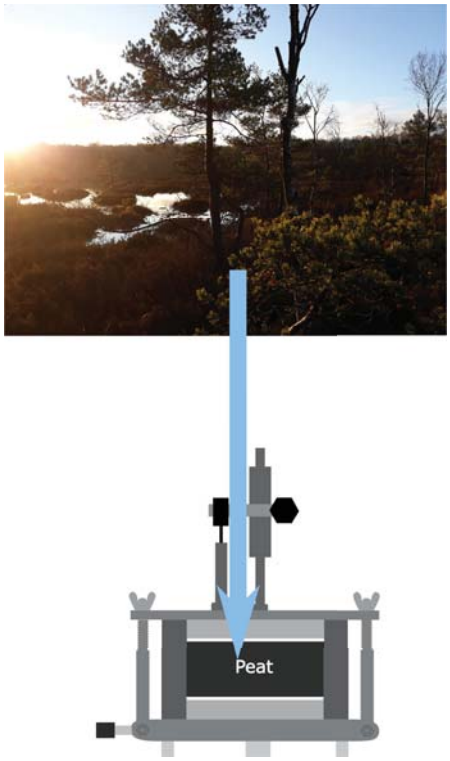

RELATIONSHIP BETWEEN SHEAR-WAVE VELOCITY AND CONSOLIDATION PARAMETERS OF PEAT

OSKAR MARKSTRÖM

Geotechnical Engineering

Master's Dissertation

DEPARTMENT OF CONSTRUCTION SCIENCES

GEOTECHNICAL ENGINEERING

ISRN LUTVDG/TVGT--18/5063--SE (1-66) | ISSN 0349-4977

MASTER'S DISSERTATION

RELATIONSHIP BETWEEN SHEAR-WAVE VELOCITY AND CONSOLIDATION PARAMETERS OF PEAT

OSKAR MARKSTRÖM

Supervisors: **ERIKA TUDISCO,** PhD, Geotechnical Engineering, LTH, Lund
and **MICHAEL LONG**, Assoc Professor, School of Civil Engineering, UCD, Dublin.

Examiner: Professor **OLA DAHLBLOM**, Dept. of Construction Sciences, LTH, Lund

Printed by V-husets tryckeri LTH, Lund, Sweden, August 2018 *(Pl)*.

For information, address:
Geotechnical Engineering, Dept. of Construction Sciences,
Faculty of Engineering LTH, Lund University, Box 118, SE-221 00 Lund, Sweden.

Homepage: www.geoteknik.lth.se

Abstract

There is a need of developing methods for evaluating material parameters for peat. It is hard and costly to obtain undisturbed samples for laboratory testing of the peat. Therefore, in this thesis the possibility of using in situ measurements of the shear wave velocity for first order estimates of the consolidation parameters has been investigated. In earlier work, relationships have been found between the shear wave velocity and consolidation parameters for Norwegian clay.

One of the biggest difficulties with peat is the large compressibility making it a difficult soil for construction work and it is avoided if possible. It is characterised by its high water content. In order for the soil to be accumulated there needs to be a high amount of rainfall and poor drainage. The high water content explains why the pressure wave velocity was not analysed in this thesis. This body wave, which controls the oedometer modulus, propagates in water making the water content the dominating factor determining the pressure wave velocity in peat. There is no shear resistance in water making the shear wave velocity more suitable to use in peat.

In the study, the peat was compressed in an oedometer using a constant rate of strain. This allows for a valuable understanding of the primary compression, which is formed as the effective stress increases. The peat has been characterised according to the extended version of the von Post scale. That includes determining its level of humification, fibre content and water content. The data in this thesis is from three different sites, referred to as Ageröds mosse, Färgelanda and Mullsjö.

The shear wave velocity is linked analytically to the shear modulus and the density of the soil. Furthermore, it has been shown it is a function of the void ratio and the current state of stress. It has been measured at the three sites by using Down hole method. Generally, it was seen to increase with depth, which can be expected since one of the controlling factors is the vertical effective stress.

The compression parameters relevant for this study is M_0, M_L, m and σ'_c. Since the unit weight of peat is close to the one of water the preconsolidation pressure can sometimes be very low. It was the case in this study where σ'_c could not be identified as well as M_0. However, both M_L and m were evaluated from the 13 oedometer tests. There was no strong correlation with V_s identified, although a weak indication for M_L was observed.

Keywords: shear wave velocity, peat, constant rate of strain, consolidation parameters, von Post

Acknowledgements

This work, marking the end of five years of studies in Lund, has been performed at the Department of Construction Sciences at LTH in cooperation with University College Dublin.

I would like to send a big thanks to my supervisors Erika Tudisco from the department and Michael Long from UCD for answering my questions and guiding me during this project. I would also like to express my appreciation to geoconsultant Andrew Trafford for the field work performed, professor Dan Hammarlund at the Department of Geology for lending equipment for the field tests and Research Engineer Jessica Dahlström at the Department of Construction Sciences for assistance in the laboratory.

Finally, I am grateful for my friends and family supporting me during this semester and throughout my time at Lund University making these years unforgettable.

Oskar Markström

Lund, June 2018

Notations

a_v	coefficient of compressibility
A	cross-sectional area
c_v	coefficient of consolidation
C_α	secondary compression index
C_c	compression index
e	void ratio
e_0	initial void ratio
$\bar{e}$	average void ratio
E	young´s modulus
G	shear modulus
$G_{\max}$	small strain shear modulus
h	thickness
k	coefficient of permeability
m	modulus number
m_s	mass solids
m_w	mass water
M	elastic modulus
$p_{vy}{}'$	yield stress
s_u	undrained shear strength
t	time
u	pore water pressure
u_b	pore water pressure at the bottom of the sample
V	volume
V_p	pressure wave velocity
V_s	shear wave velocity
$V_{\bar{s}}$	volume of the solids
w	water content
z	depth

γ_w	unit weight of water
δ	settlement
ϵ	strain
μ	relative magnetic permeability
σ'	effective stress
σ'_0	in situ stress
σ'_c	preconsolidation pressure
σ'_v	effective vertical pressure

Table of Contents

1 Introduction

1.1 Background

The settlements are the biggest concern regarding construction on peat. It is, therefore, of big interest to determine the consolidation parameters. This can be achieved by performing oedometer tests (Carlsten 1988). In addition to the high compressibility of the material, peat has low shear strength, usually in the range of 5-20 kPa and high water content. The normal practice is to avoid peat because of its weak nature but because of the shortage of suitable land it is not always possible to do this (Huat et al. 2014). For construction on an area with peat soil, this can either be excavated or preloaded. At most times construction is not made solely on the peat without preparing it first. By preloading the settlements can be reduced considerably. It is also possible to use piles from which the load is transferred to firm soil below the peat layer or to the bedrock.

Peat is characterised by a high content of organic matters and is derived mainly from plant remains. The colour is usually dark brown or black. It is defined as a soil with an organic content that is larger than 35 %, but in geotechnical applications the organic content should exceed 75 % for it to be addressed as peat. In order for peat to be created the plant remains have to be preserved under limited access to air and at high water content. Areas with high amounts of rainfall combined with poor drainage is suitable for accumulation of the soil (Huat et al. 2014). It is often said that the annual rainfall must exceed 1200 mm and that the peat grows 1 mm per year. The depth of the peat is limited by the fact that all peat deposits in Europe, Asia, Canada and USA have accumulated since the last ice age.

The knowledge about the geotechnical properties of peat is limited, compared to what is known about clay. Vesterberg et al. (2016) state that there is a need to develop methods to evaluate material parameters for peat. Obtaining undisturbed samples for the material is challenging. Therefore, the possibility of using in situ tests to obtain first order estimates of consolidation parameters for peat is investigated.

The small strain shear modulus is linked analytically with the shear wave velocity, V_s via the density. Although there is no analytical relationship between V_s and consolidation parameters, it is plausible to find an empirical one. L´Heureux & Long (2017) found a relationship between V_s and consolidation parameters for Norwegian clay. V_s can be of more significant use for peat compared to other soils as the P-wave velocity, V_p, is mainly controlled by the high water content of the peat.

1.2 Objective and limitations

The purpose of this work is to obtain consolidation parameters from CRS-tests and compare them to in situ measurements of V_s in order to investigate if a relationship between the consolidation parameters and V_s can be found.

While V_s will be evaluated for the full peat depth it is hard to obtain block samples for high depth resulting in fewer and more shallow samples to be used in oedometer test. Therefore, a comparison can only be made for a limited region and the data need to be complemented for a meaningful regression analysis. The oedometer testing procedure is time demanding since the

peat samples are to be deformed around 80 %. Considering that most of the block samples are shallow it is worth noting that the accuracy of V_s can be a bit lower at a shallow depth.

The study will not go into detail on the reasons for existence for a relationship. Thus, the different aspects of peat that affect the shear wave velocity is only discussed briefly.

1.3 Methods

Initially a literature review was carried out to gain knowledge about the compressional behavior of peat, in situ shear wave testing and oedometer tests.

As part of the project, field work was performed at Ageröds mosse which is a peat bog in Scania, Sweden. V_s was determined every 0.1 meters using "Down hole method". By using a Russian sampler it was possible to obtain samples for evaluation of the water content at the same depths as V_s measurements. The core sample gained from the Russian sampler was also used to categorise the peat according to von Post scale of humification.

Block samples were extracted from the site in order to evaluate compression parameters in the laboratory. Constant rate of strain (CRS) tests were performed in the laboratory at LTH in Lund. The results from the field tests were compared to the values obtained from the laboratory. V_s data was also available from two other sites from which one block sample each was used to evaluate the consolidation parameters.

1.4 Disposition

The thesis is containing chapters treating the following:

Chapter 2: *Material characterisation* – The material parameters and water content obtained from the tests are defined in this chapter.

Chapter 3: *Methods* – A description of the methods used in the work.

Chapter 4: *Geophysics* – Fundamental information about shear waves and GPR, which is a commonly used for profiling peat. Earlier research on the relationship between shear waves and material parameters are also provided.

Chapter 5: *Field work* – The different field sites are described along with the obtained information of the sites from the von Post-logging.

Chapter 6: *Results* – The results from field testing and laboratory work are shown.

Chapter 7: *Discussion and conclusions* – The results are discussed and conclusions from the work are stated.

2 Material characterisation

The compression in peat is very large compared to soft clay and silt when the effective stress is increased. Total compression can be divided into a primary compression which is formed during the increase of effective stress and a secondary compression which is observed at constant effective stress.

Primary compression, or consolidation, is a result of loading and dissipation of excess pore water pressure. Unlike for mineral soils, the consolidation process is rapid for peat, it takes only a few minutes until the primary compression has developed in the laboratory (Huat et al. 2014). That is valid for traditional incremental load testing, for constant rate of strain a continuous excess pore water pressure will be created. The primary consolidation is active until the increase of pore water pressure, due to the increase of load, is neutralised.

The compression index C_c is given by:

$$C_c = \frac{\Delta e}{\Delta log\ \sigma'_v} \tag{2.1}$$

That means C_c is the slope of the plot of void ratio, e, and the logarithm of vertical effective stress in kPa as is shown in Figure 2.1. Huat et al. (2014) claim that, C_c, ranges from 2 to 15 for peat.

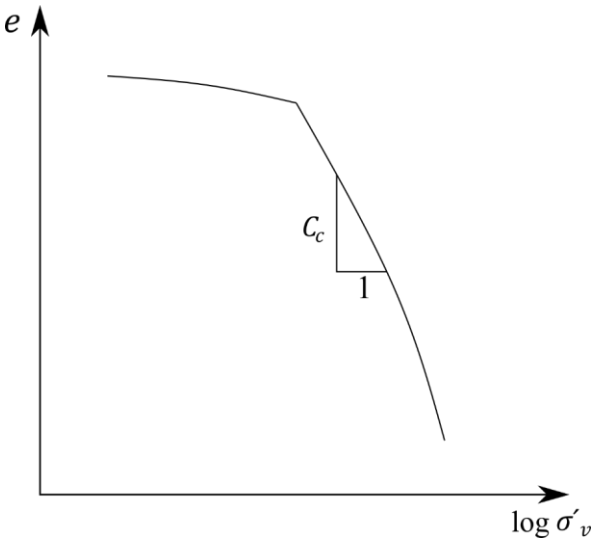

Figure 2.1: Illustration of the definition of C_c in a plot of log σ'_v against e.

The secondary compression in peat is understood to occur as the fibres are further decomposing. The decomposition rate and thus the compression rate is slower after the primary compression is finished. The secondary compression is also developing due to reorganisation of the structure to a denser form. The secondary compression is although the larger part of the settlements compared to primary compression (Huat et al. 2014).

Olsson (2010) expresses the secondary compression index C_α as:

$$C_\alpha = \frac{\Delta e}{\Delta \log(t)} \tag{2.2}$$

where t is the time. As a soil sample is loaded, the void ratio decreases with time as shown in Figure 2.2.

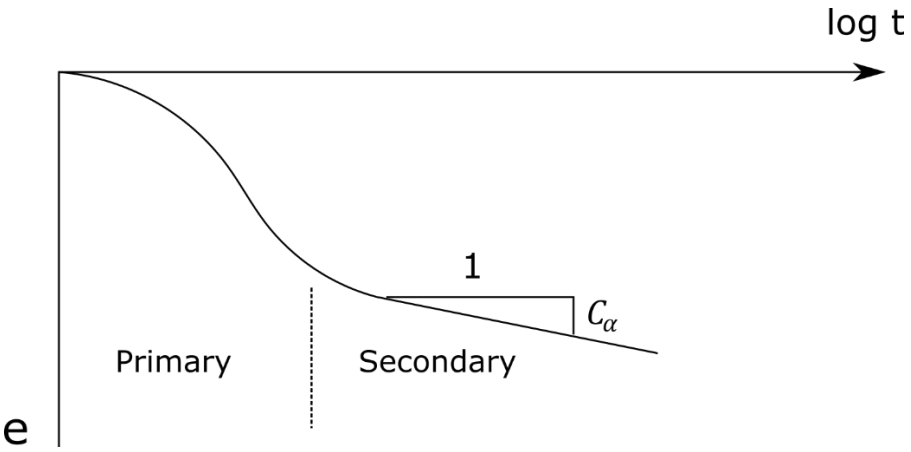

Figure 2.2: Consolidation curve – recreation of Olsson (2010).

Void ratio is defined as the volume of pores, empty or filled with water, to the volume of solids according to:

$$e = V_v / V_{\bar{s}} \tag{2.3}$$

Where V_v is the volume of the void and $V_{\bar{s}}$ is the volume of the solids.

The void ratio for peat usually varies between 7 to 25 (Huat et al. 2014). It is higher for fibrous peat since the compressible bendable hollow fibres form an entangled network of particles, resulting in high water content (Mesri and Ajlouni 2007).

The in situ void ratio is a factor determining the compressibility of soil and is high for fibrous peat. Water is squeezed out from the fibres during both primary and secondary compression resulting in high compressibility (Mesri and Ajlouni 2007).

The highest ratios between secondary compression index and compression index amongst geotechnical materials are found for peat (Mesri and Ajlouni 2007). Fox et al. (1993) claim that several studies of clay suggest that the ratio between C_α and C_c is constant. It has been shown that C_α increases linearly with C_c for Leda clay as well as Chicago blue clay and Mexico City clay. However, they found no linear relationship for peat.

Since the unit weight of peat is around that of water the effective stress σ' is small and hard to observe from a consolidation test (Mesri et al. 1997). It is also hard to detect the beginning of secondary compression since the primary compression occurs swiftly according to Yulindasari (2006) study (as referred to in Huat et al. 2014).

Apart from primary compression, which is formed as the peat consolidates, and the secondary compression, it exists an immediate elastic compression. This is formed because of compression of gas within pores and compression of soil grain. The settlements compared to mineral soils are larger and they can take much longer time as well as a result of secondary compression (Huat et al. 2014).

Void ratio is one of the parameters determining permeability in soil. Permeability affects the rate at which a soil consolidates under the influence of increased load. Other parameters determining permeability are size and shape of flow channels where large pores and straight

flow channels gives large permeability. There is a big anisotropy in permeability for fibrous peat (Mesri and Ajlouni 2007). The permeability of uncompressed peat is considerably higher than for silt and clay, normally around 1000 times higher. However, the permeability rapidly decreases as load is applied to the peat (Mesri and Ajlouni 2007). This can be observed during CRS testing as the pore water pressure can increase rapidly when the peat is compressed.

2.1 Oedometer modulus

The oedometer modulus is often used for settlement calculations. It is obtained from an oedometer test and is divided into three different parameters depending on the pressure acting on the soil, illustrated in Figure 2.4. M_0 is valid for loading lower than the preconsolidation pressure, σ'_c, defined in Section 2.2 and M_L is used for pressures between σ'_c and σ'_L. Furthermore, when the pressure exceeds σ'_L the oedometer modulus is expressed as a function of the modulus number, m.

In order to derive a formula for the settlements, M is first defined as the derivative of σ' with respect to the strain, ϵ.

$$M = \frac{d\sigma'}{d\epsilon} \tag{2.4}$$

$$d\epsilon = \frac{d\sigma'}{M} \tag{2.5}$$

$$\epsilon = \int_{\sigma'_0}^{\sigma'_0+\Delta\sigma} \frac{d\sigma'}{M} \tag{2.6}$$

The settlements are then calculated as:

$$\delta = \int_0^h \epsilon dz \tag{2.7}$$

Inserting (2.6) into (2.7):

$$\delta = \int_0^h \int_{\sigma'_0}^{\sigma'_0+\Delta\sigma} \frac{d\sigma'}{M} dz \tag{2.8}$$

For $\sigma' > \sigma'_L$, M is a function of σ', it is therefor also a function of the depth z. Let:

$$M = m\sigma'_j \left(\frac{\sigma'}{\sigma_j}\right)^{1-\beta} \tag{2.9}$$

Where m is the modulus number, β is the stress exponent and σ'_j=100 kPa. The settlement thus becomes:

$$\delta = \int_0^h \frac{1}{m\beta} \left[\left(\frac{\sigma'_0 + \Delta\sigma}{\sigma'_j}\right)^{\beta} - \left(\frac{\sigma'_0}{\sigma'_j}\right)^{\beta} \right] dz \tag{2.10}$$

By using numerical integration the settlement can be calculated as the area below the ϵ-curve as is shown in Figure 2.3.

$$\delta = \sum h_1 \frac{1}{m\beta}\left[\left(\frac{\sigma'_0 + \Delta\sigma}{\sigma'_j}\right)^{\beta} - \left(\frac{\sigma'_0}{\sigma'_j}\right)^{\beta}\right] \tag{2.11}$$

The modulus number, m, is evaluated according to Figure 2.4.

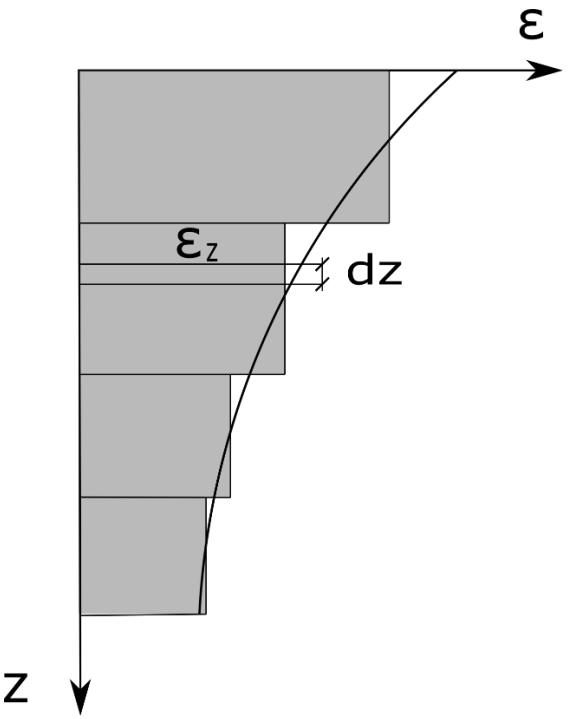

Figure 2.3: Illustration of the settlement by using numerical integration. Reconstruction of Sällfors (1975).

If $\beta = 1$, $M = m \cdot \sigma'_j = constant$ and the settlement can be calculated as:

$$\delta = \sum_{i=1}^{n} h_i \frac{\Delta\sigma_i}{M_i} \tag{2.12}$$

which state how the settlement depends on M when the soil is divided in sections (Sällfors 2013).

M_0 and M_L are evaluated from an oedometer test and are by principle varying according to Figure 2.4. This figure also illustrates the importance of a good estimate of σ'_c for an accurate settlement analysis as Sällfors (1975) highlights. Since the compression modulus is defined by:

$$M = \frac{d\sigma'}{d\epsilon} \tag{2.13}$$

the compression modulus is evaluated from the stress-strain curve. There is a risk of a big spread of the value of $d\sigma'/d\epsilon$ if it is only based on two consecutive datapoints. Thus, it is recommended using a linear regression of 5-10 consecutive values (Sällfors & Andréasson 1986). The number of datapoints used is determined through analysing the scatter of the data, where a large scatter will require more datapoints for the linear regression.

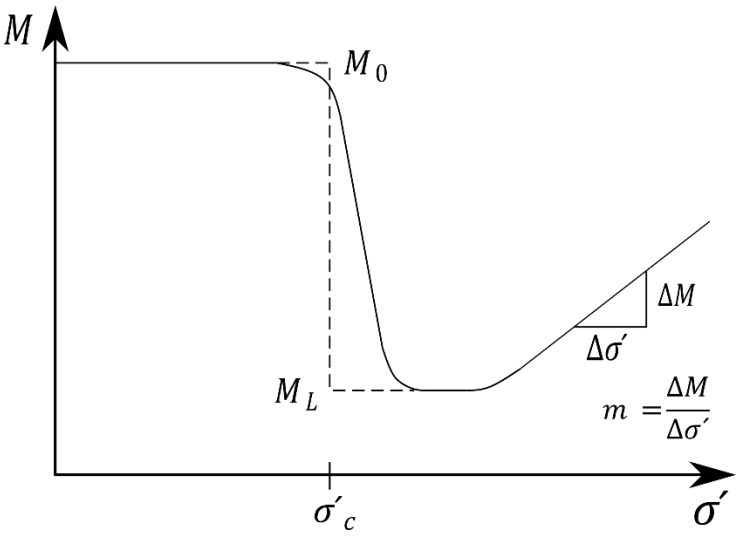

Figure 2.4: Variation of oedometer modulus with increasing effective stress. Based on Sällfors & Andréasson (1986).

Because of the heterogeneous nature of peat standard, 20 mm thick samples may not be suitable for peat. A thicker sample should be used but a large sample is not practical and the test duration is prolonged (Long & Boylan 2013). There can be difficulties in handling peat and obtaining a representative sample due to high heterogeneity of the material as can be seen in Figure 2.5.

Figure 2.5: Timber fragment illustrating the heterogeneity of peat.

2.2 Preconsolidation pressure

When there is sedimentation the effective stress increases as the material is accumulating. The increasing effective stress results in deformation. If the sedimentation is stopped and the thickness decreases for instance due to erosion that would reduce the effective stress. Since a big part of the deformation is plastic there will only be a small negative strain. The effective stress can also decrease if the groundwater level increases.

If there is once more an increase in loading, as is shown in Figure 2.6, the deformation will at first be small – until the preconsolidation pressure σ'_c, which is the highest stress the soil has reached before, is reached. At that point the compression is increasing rapidly again. If the current effective stress σ'_0 is equal to σ'_c, the soil is normally consolidated. If σ'_0 is smaller than σ'_c the soil is overconsolidated. σ'_c is of big importance for clays but are not as important for frictional soils (Sällfors 2013). Evaluation of preconsolidation pressure can be harder to measure for peat compared to clay as it is often very small.

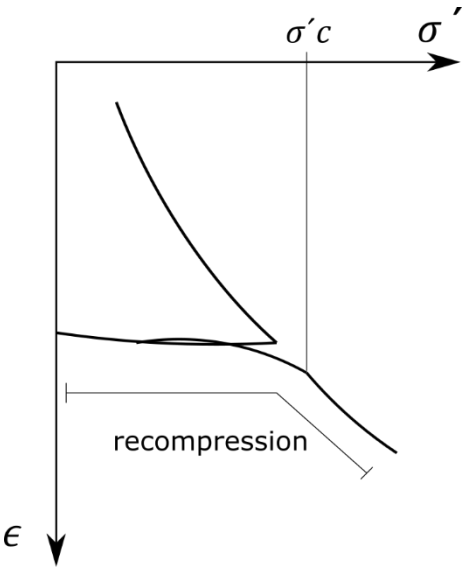

Figure 2.6: Stress is removed and then again applied to a soil sample. Based on Sällfors (2013).

2.3 Water content

The water content in peat is high compared to most other soils, this allows for a large consolidation. Moreover, since both the water content and the compression index are controlled by the composition and the structure of the soil there should be a direct correlation between them (Mesri and Ajlouni 2007).

When comparing water content to shear wave velocity, V_s in peat, there is usually a reverse relationship. This is reasonable considering that shear waves do not propagate in water. L'Heureux & Long (2017) concluded that V_s is likely strongly controlled by water content and vertical effective stresses in Norwegian clays.

The water content, w, of the soil is given by:

$$w = m_w/m_s \tag{2.14}$$

Where m_w is the mass of the water and m_s is mass of the solid. This is calculated by weighing the test specimen before and after being in the oven for at least 24 hours at $105\ °C$.

3 Methods

3.1 Von Post-logging

It is important to describe the fundamental characteristics of the peat such as the level of humification and the water content. That is because the mechanical properties can differ considerably for peat (Vesterberg et al. 2016). During humification there is a loss in organic matter, it leaves either in gas or liquid form. That implies a change in structure and chemical state.

The peat has been classified according to an extended version of the von Post scale, the samples were obtained from a Russian Sampler. The original method was developed by Lennart von Post in order to classify the Swedish peat reserve as Sweden had a shortage of fuel during World War 1. Between 1917 and 1924 the work was performed to characterise the peat, which can be used as an alternative fuel. Although the method was developed in order to use the peat as fuel, it is also applicable for geotechnical purposes (Carlsten 1988). The extended version of von Post used in this field work was established by Hobbs (1986). It is used to characterise the peat column at regular intervals.

The different stages of the classification used for this work is shown in Table 3.1.

Table 3.1: Stages for classification of the peat.

Stage	***Description***				
1	**Plant types**				
2	**Humification**	H1 (undecomposed) ⟶ H10 (entirely decomposed)			
3	**Water content**	B1	B2 <500%	B3 >500%	B4 >1000%	B5 >2000%
		Dry ⟶ Wet			
4	**Fine fibres (<1mm)**	F0 None	F1 Low	F2 Moderate	F3 High	
5	**Coarse fibres (>1mm)**	R0 None	R1 Low	R2 Moderate	R3 High	
6	**Wood & Shrub**	F0 None	F1 Low	F2 Moderate	F3 High	

The level of humification is characterised based on a 10 level scale, which spans from completely undecomposed peat to completely decomposed peat (Von Post & Granlund 1926).

$\boldsymbol{H_1}$**:** Completely undecomposed, the plant structure is easily identified, no content of amorphous material and there is only clear, colourless water when the sample is squeezed.

$\boldsymbol{H_2}$: Minimum decomposition, the plant structure is easily identified, no content of amorphous material and the water is slightly yellow when squeezed.

$\boldsymbol{H_3}$**:** Very small decomposition and the plant structure is moderately identifiable. There is a small content of amorphous material and the water is brown, muddy and there is no peat squeezed out.

$\boldsymbol{H_4}$**:** Small decomposition, the plant structure is hard to identify. There is some content of amorphous material and the water is dark brown, muddy. There is no peat squeezed out.

$\boldsymbol{H_5}$**:** Average decomposition and the plant structure is detectable, but only vague. There is a substantial content of amorphous material. Some peat is squeezed out and the water is muddy.

$\boldsymbol{H_6}$**:** Rather significant decomposition and the plant structure is inexplicit. There is a substantial content of amorphous material. Around one third of the peat is squeezed out and the water is dark brown.

$\boldsymbol{H_7}$**:** The decomposition is significant, and the plant structure is faintly identifiable. The content of amorphous material is high. Around half of the peat is squeezed out and if there is water it is dark brown.

$\boldsymbol{H_8}$**:** Very significant decomposition, the plant structure is very inexplicit, high content of amorphous material. Around two thirds of the peat is squeezed out and the water is pasty.

$\boldsymbol{H_9}$**:** Almost completely decomposed, the plant structure is almost impossible to distinguish. Almost all the peat is squeezed out as an even paste.

$\boldsymbol{H_{10}}$**:** Completely decomposed and the plant structure is not visible. All the peat is squeezed out and no free water can be observed.

The fibre content, stages 4-6, was determined in the field just like the humification. However, the water content, stage 3, was measured in the laboratory.

Samples, for characterisation, was obtained by using a Russian sampler. The sampler has been a commonly used corer for peat soils since the mid 20th century (Franzén & Ljung 2009). The corer is pressed down into the peat. At the point when the chamber of the sampler is at sufficient dept the T-handle is rotated 180 degrees to enclose the sample. On withdrawal, two undisturbed quarter cylindrical samples are obtained (Jowsey 1965). However, in the field work in question half-cylindrical samples was obtained. The Russian sampler used in the work is shown in Figure 3.1.

Figure 3.1: The Russian sampler used with peat in the steel chamber.

3.2 Down hole method

In order to measure the shear wave velocity, V_s, a portable downhole sonde is connected to a seismograph. In Figure 3.2. the seismograph used in the field work is shown. V_s is observed at different depts of the vertical peat column. Shear waves are generated by impacting a hammer on a small plastic block buried at a shallow depth. A trigger inside the source starts recording the traces as the hammer inflicts the source (Trafford & Long 2016).

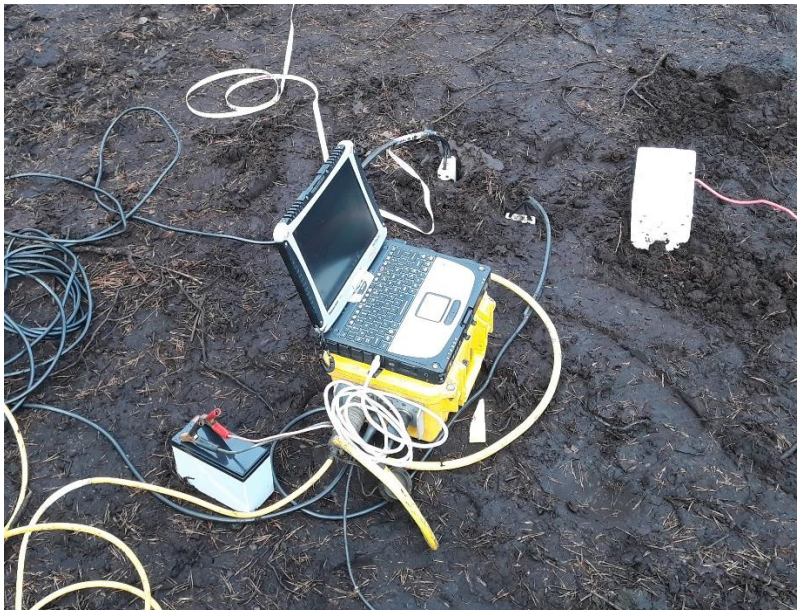

Figure 3.2: Seismograph system, setup from Ageröds mosse.

Vertical shear waves are detected by a geophone at increasing depths within a borehole. The source is on the ground and the shear waves are transmitted subvertically and are detected at different depths. This is illustrated in Figure 3.3. For this work, the soil extracted from the borehole is previously logged according to the von Post scale.

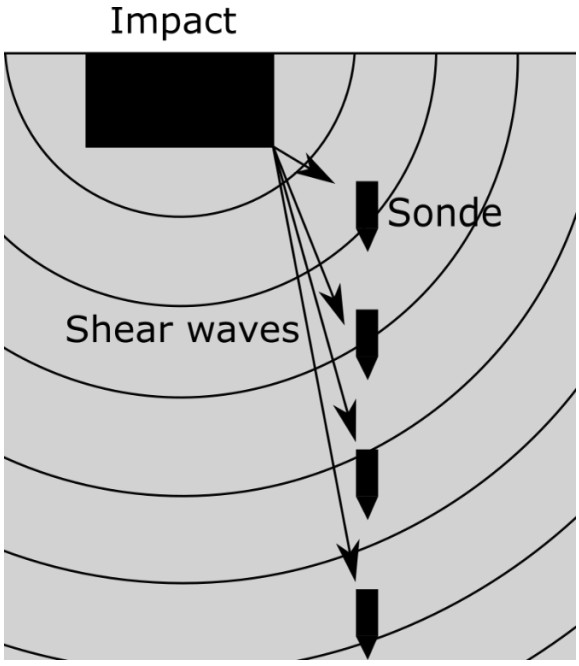

Figure 3.3: Basic principle of "Down hole method". Based on Trafford (2017).

The sonde is pushed into the peat to record the shear waves that are transmitted. The sonde is similar to the cone used in Seismic Cone Penetration Testing. In addition to the equipment needed for generating and receiving shear waves, a seismograph is required. For the field work at the three different sites a Geometrics Geode is used (Trafford 2017).

Ideally there would be multiple receivers close to one another in order to record interval velocities. This has been tested, but the transmitted velocities could not be decided because of direct coupling between the receivers. Therefore, only one receiver is used and the direct transmission is measured (Trafford 2017).

In order to make the borehole where the sonde can be fitted, a Russian sampler can be used. According to Trafford (2017) the presence of push rods while doing shear waves measurements posed a problem as disturbance occurs from the wind and channel waves along the bars, which makes it hard to accurately detect the shear wave first arrivals. Thus, the bars must be removed after they have pushed down the sonde to maximal peat depth. In order to get the shear wave profile the sonde is moved up at a constant interval, 0.1 meters as suggested by Trafford (2017).

A trigger within the block source detects when the block is struck, see Figure 3.4. The recordings start on that signal. There is a reference geophone placed at a fixed distance from the source to account for any errors in the recordings start time. The block source is kept at a firm contact with the ground. The source is struck at two different directions to obtain opposing phase records. The result is then assembled into a single record accurately identifying the shear wave first arrivals (Trafford 2017).

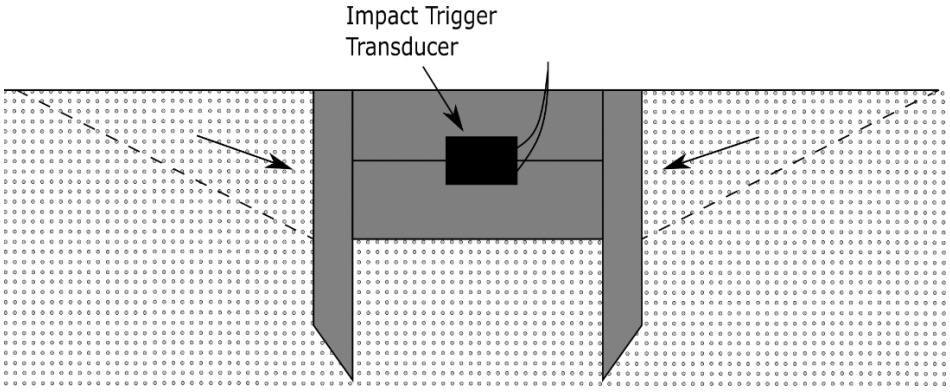

Figure 3.4: Trigger block and direction of impact. Based on Trafford (2017).

3.2.1 Elastic wave source

In order to generate elastic shear waves a source needs to impact the soil. Milsom & Eriksen (2011) denotes the sledgehammer as useful for small-scale investigations, as can be seen in Figure 3.5. The energy is almost always sufficient for refraction work at depths ranging from 10-20 meters. The effectiveness is however dependent on ground conditions and according to Trafford & Long (2016) the S-wave velocity in peat is low compared to other materials. The sledgehammer impacts a flat plate that abruptly stops the hammer creating an easily distinguishable wave traveling through the soil. Nowadays rubber discs are usually favoured over noisy aluminium or steel plates (Milsom & Eriksen 2011).

Figure 3.5: A sledgehammer used as the source in the small-scale investigation at Ageröds mosse.

For larger field investigations a more powerful source can be used. A crane can raise a weight of hundreds of kilograms to at least four meters. As the weight powerfully hit the ground the support rebounds (resulting in additional seismic waves) thus demanding a minimum height of four meters. Another method is stretching elastic bands so that the weight hits the ground at a high velocity. The technique called Propelled Energy Generator is performed from an elevation of just half a meter (Milsom & Eriksen 2011).

3.2.2 Geophone

Detectors for land based seismic waves are called geophones, which convert mechanical energy to electrical energy. For marine applications, hydrophones are used (Milsom & Eriksen 2011). As a seismic wave moves the skeleton of particles in the ground, a wire coil moves in the magnetic field inducing a voltage. It is the relative motion between the case and the coil that causes the voltage. The velocity of the deformation of soil particles is the measured parameter, as the velocity of the movement of the coil determines the current flowing. The different components of a geophone are illustrated in Figure 3.6. On a practical note, a geophone needs to be resilient as it must be able to withstand both water and dust. Furthermore, because of the use in different locations it cannot be sensitive to temperature variations (Gadallah & Fisher 2009).

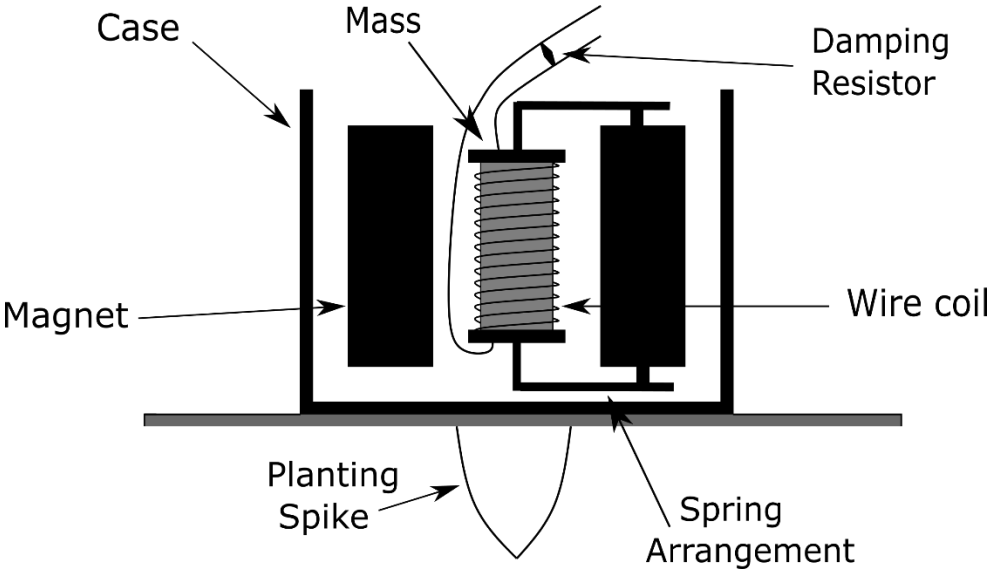

Figure 3.6: Components of a geophone. Based on Gadallah & Fisher (2009).

3.3 Incremental load

Incremental load test is the standard oedometer test where the sample is maintained under a single load for 24 hours. During an oedometer test, the lateral stain is prescribed to zero, only strain in the vertical direction is allowed. With this method, it is not possible to identify the exact value of σ'_c (Korhonen & Lojander n.d.). By applying incremental load it is possible to evaluate the secondary compression. It can be of big importance as Huat et al. (2014) states the creep part of the compression is a larger part of the total settlement for peat compared to other soils.

For evaluation of σ'_c, according to Casagrande´s method, a graph is made with σ' at the x-axis and the compression as percentage of the initial sample height is on the y-axis in a logarithmic scale. The point on the oedometer curve where the radius is smallest is chosen and a tangent is drawn through the point as well as a line parallel to the abscissa, see Figure 3.7. A bisector is drawn between the tangent and the horizontal line. The point where the bisector is intersected to the extended linear part of the virgin curve is σ'_c (Sällfors & Andréasson 1986).

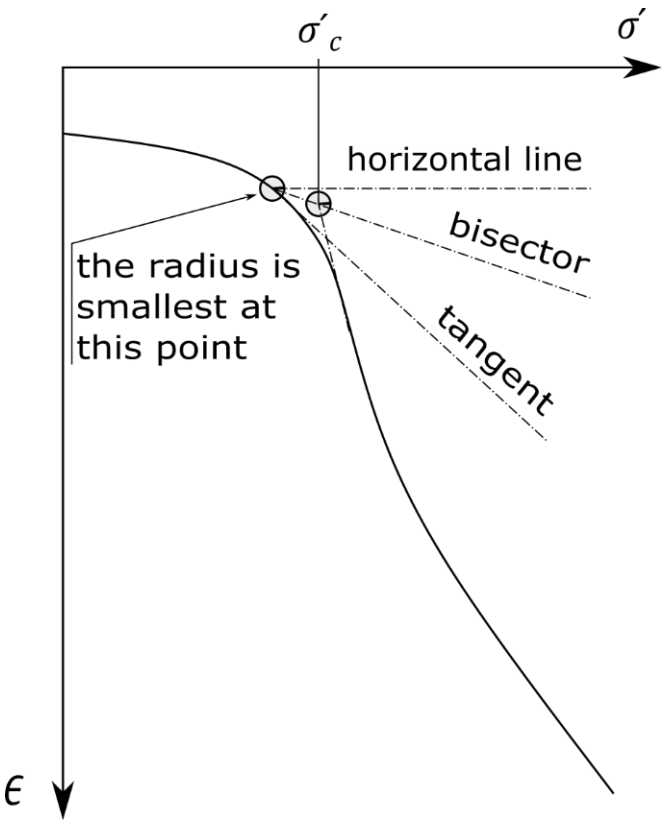

Figure 3.7: Oedometer curve for evaluation of σ'_c where the σ´-axis is logarithmic and ϵ-axis is linear. Recreation of (Sällfors & Andréasson 1986).

For $\sigma' > \sigma'_c$:

The part of the oedometer curve where the stress is higher than the preconsolidation stress can often be approximated linearly. If this approximation is valid there is only one parameter describing the curve, the modulus number, m, apart from the preconsolidation pressure. In order to determine m the relative compression $\Delta\epsilon$ is calculated. It is defined as the compression as the stress increases from σ'_j to $2.7\sigma'_j$ where σ'_j is advised to be set to 100 kPa. If σ'_c > 100 kPa the virgin curve is extended and σ'_j is prescribed to 100 kPa at the extended part. It is now possible to calculate m as (Sällfors & Andréasson 1986):

$$m = \frac{1}{\Delta\epsilon} \tag{3.1}$$

3.4 Constant rate of strain

Constant rate of strain, CRS, is a younger method compared to traditional incremental loading for determining the compressional parameters. For practical reasons it is the more suitable method to be used. It is faster and allows for a more complete evaluation of the compressional behavior. On the downside it cannot be used to determine the secondary compression. A third method, triaxial testing, can also be used to evaluate the compressional properties. However, it is complicated compared to the other two methods (Sällfors & Andréasson 1986).

CRS was chosen over incremental load as the method to determine the compression parameters. Korhonen & Lojander (n.d.) has argued that there are problems regarding the evaluation of the preconsolidation pressure for incremental load testing. It is not possible to

determine an exact value. Yong & Townsend (1986) claims that Leroueil et al. (1983) concluded that there is no unique value for preconsolidation pressure, it depends on the method used. They state, on the other hand, that the in-situ preconsolidation pressure in reality can be estimated from CRS tests for clays. That can also be done by conventional oedometer testing but they claim CRS is to be preferred. That is agreed upon by Sällfors (1975) who states that the CRS-procedure results in a value that is not only more accurate it is also obtained much faster. In addition, the secondary compression is not necessary for the basis of this work therefore CRS is used. However, since the primary compression is formed quickly for peat CRS testing may not be faster for testing this soil.

Evaluation of the preconsolidation pressure can be done from the stress-strain curve, illustrated in Figure 3.8. Sällfors (1975) recommends the following method:

The first linear part of the stress-strain curve is extended as well as the tangent of the inflexion point of the virgin curve. A line is then drawn between both of the extended lines with the base of the new line at the stress-strain curve creating an equilateral triangle. A vertical line is then drawn from the triangle displaying the value of σ'_c.

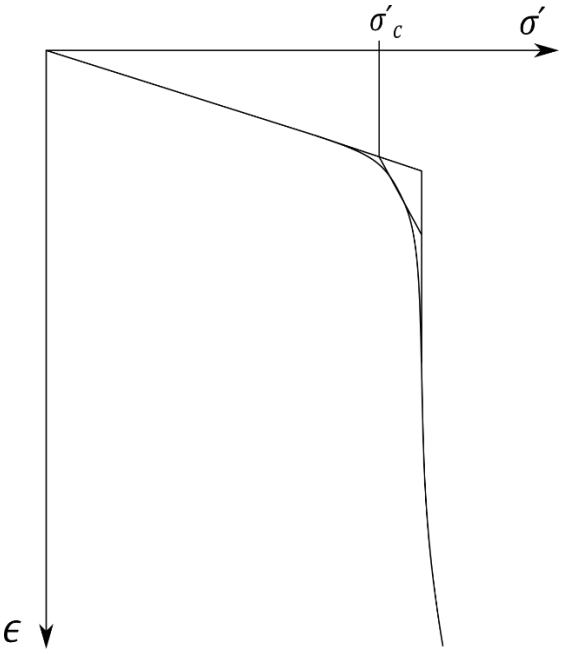

Figure 3.8: Evaluation of preconsolidation pressure. Based on Sällfors & Andréasson (1986).

The oedometer used for CRS testing consists of an oedometer ring and water pressure transducer at the lower end of the sample shown in Figure 3.9. The sample is compressed by the load from a press, the strain is then developed at a predetermined constant rate. The rate can be decided experimentally by testing different rates. The pore water pressure cannot be allowed to increase to a state where it is close to the total pressure, this can be avoided by

lowering the rate of strain. Sällfors & Andréasson (1986) states that water is only drained from above alongside a porous stone that has got the same diameter as the sample.

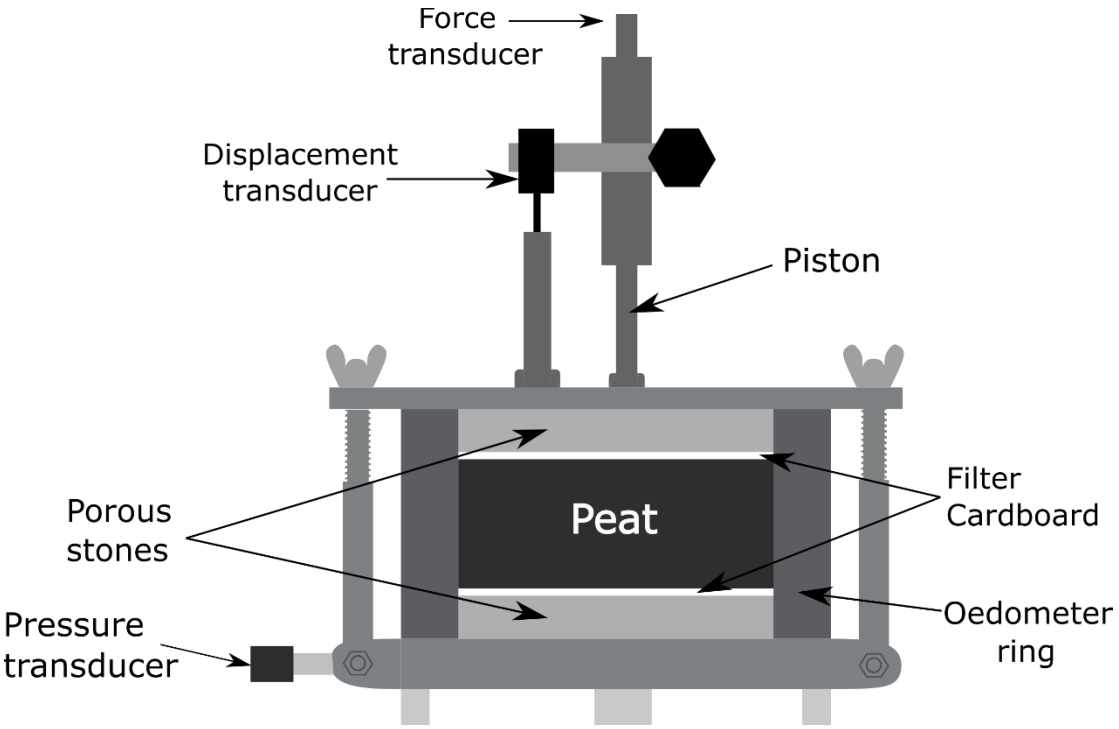

Figure 3.9: 2D-representation of the oedometer used in the laboratory tests.

From knowing the vertical load, deformation and pore pressure the effective stress (σ') and the compression (ϵ) can be calculated (Magnusson et al. 1989). This is registered at frequent time intervals during the tests (Sällfors & Andréasson 1986).

Assuming a parabolic distribution of pore pressure the effective stress can be expressed as (Sällfors 1975):

$$\sigma' = \sigma - \frac{2}{3}u_b \tag{3.2}$$

with u_b being the pore pressure at the bottom of the sample. This is valid under the assumptions below according to Smith & Wahls (1969) theoretical study.

- The soil is saturated and homogeneous
- The water and the solids are incompressible compared to the soil
- Darcy´s law applies for flow within the soil
- The soil´s lateral movement is prescribed to zero
- Stress is uniform within each horizontal plane. Differences only occur between different planes.

If these assumptions are used the non-linear partial differential equation of consolidation is:

$$\frac{\partial}{\partial z}\left(\frac{k}{\gamma_w}\ \frac{\partial u}{\partial z}\right) = \frac{1}{1+e}\ \frac{\partial e}{\partial t} \tag{3.3}$$

in which z is the depth, k is the coefficient of permeability, γ_w is the unit weight of water, u is excess pore water pressure, e is the void ratio and t is time. The relationship is established

from the continuity of flow through a soil element. Equation (3.3) can be simplified under the condition that k is a function of the average void ratio, $\bar{e}$, making it dependent of time and not depth. Thus, the equation becomes:

$$\frac{k}{\gamma_w}\ \frac{\partial^2 u}{\partial z^2} = \frac{1}{1+e}\ \frac{\partial e}{\partial t} \tag{3.4}$$

As no horizontal movement is allowed and the rate of strain is constant, the change of volume is constant and can be written as:

$$\frac{dV}{dt} = -RA \tag{3.5}$$

where V is the volume, R is the deformation in the upper surface and A is the cross-sectional area. It follows that the rate of change of average void ratio, $\bar{e}$, is:

$$\frac{d\bar{e}}{dt} = \frac{1}{V_{\bar{s}}}\ \frac{dV}{dt} = -\frac{RA}{V_{\bar{s}}} = -r = constant \tag{3.6}$$

where $V_{\bar{s}}$ is the volume of solids and:

$$\bar{e} = \frac{1}{H}\int_0^H e dz \tag{3.7}$$

The void ratio is a linear function of time based on (3.6) and (3.7) and is written as:

$$e = gt + e_0 \tag{3.8}$$

in which g is a function of depth and e_0 is the initial void ratio. Smith & Wahls (1969) claim that it is not practical to decide g. Because of that it is not possible to solve (3.4), instead a linear function is assumed which makes (3.8):

$$e = e_0 - rt\left[1 - \frac{b}{r}\left(\frac{z - 0.5H}{H}\right)\right] \tag{3.9}$$

where b is a constant depending on the variation of the void ratio as a function of depth and time. Likewise, b/r depends on the variation of the void ratio, but only varies with depth. It can vary between 0 to 2 where $b/r = 0$ means that the void ratio is constant with depth. If $b/r = 2$ the void ratio is constant at the end of the sample. A solution to the differential Equation (3.4) is obtained as (3.9) defines the void ratio and the following boundary conditions are used:

$$u(0,t) = 0 \tag{3.10}$$

$$\frac{\partial u}{\partial z}\,(H,t) = 0 \tag{3.11}$$

The solution for the case that the void ratio is constant with depth, $b/r = 0$ is:

$$u = \frac{\gamma_w r}{k(1+\bar{e})}\left(Hz - \frac{z^2}{2}\right) \tag{3.12}$$

The analogous solution for $b/r \neq 0$ is more complicated and Smith & Wahls (1969) advises to use a simplified form. It is done by assuming that $(1 + e)$ can be replaced by $(1 + \bar{e})$ in (3.4). The solution for $b/r \neq 0$ then becomes:

$$u = \frac{\gamma_w r}{k(1+\bar{e})}\left[\left(Hz - \frac{z^2}{2}\right) - \frac{b}{r}\left(\frac{z^2}{4} - \frac{z^3}{6H}\right)\right] \tag{3.13}$$

From this it is possible to evaluate the pore pressure at the bottom of the sample where $z = H$, where it is measured during a CRS test. Hence, (3.13) becomes:

$$u_{z=H} = u_b = \frac{\gamma_w r H^2}{k(1+\bar{e})}\left[\frac{1}{2} - \frac{b}{r}\left(\frac{1}{12}\right)\right] \tag{3.14}$$

The definition of coefficient of consolidation, c_v, by Terzaghi (1943) is:

$$c_v = \frac{k(1+e)}{a_v \gamma_w} \tag{3.15}$$

where a_v is the coefficient of compressibility. C_v governs the rate at which a soil compresses when subjected to increasing load. In this expression the unknown is k. According to Smith & Wahls (1969) equations (3.14) and (3.15) can be combined to evaluate c_v at any given void ratio from a CRS test when u_b is measured:

$$c_v = \frac{r H^2}{a_v u_b}\left[\frac{1}{2} - \frac{b}{r}\left(\frac{1}{12}\right)\right] \tag{3.16}$$

Evaluating c_v can be valuable for analysing the result of an CRS test, preferably presented as a plot against effective stress.

According to Korhonen & Lojander (n.d.) the CRS-tests usually last one to two days. The results are ready quickly since the tests and processing of the data is automatised at most times. However, the results from the tests need to be reduced in order to use them in settlement calculations.

In the work of Long & Boylan (2013) the effects of four different strain rates were investigated from four different sites for peat. The authors state that for slower strain rates creep may influence the results. It is concluded that the test rate does not affect the results of M_0 or the compression index C_c. To separate elastic from plastic behavior the term yield stress, $p_{vy}{}'$, can be used. It has been found that it is affected by strain rate for clay and Long & Boylan (2013) found a similar relationship for peat. It was found that $p_{vy}{}'$ increases as the strain rate increases. A higher rate of strain also results in higher preconsolidation pressure since the stress-strain relation is time dependent (Sällfors & Andréasson 1986).

4 Geophysics

4.1 Shear waves

Shear waves, S-waves, is a type of seismic wave that consists of acoustic energy. For low-energy waves the material is left unchanged, it is therefore elastic which is the case for geophysical applications. S-waves are in addition to pressure waves, P-waves, referred to as elastic body waves. For P-waves the molecules oscillate backwards and forwards in the direction of the wave propagation, as is shown in Figure 4.1. That results in a velocity higher than for shear waves (Milsom & Eriksen 2011).

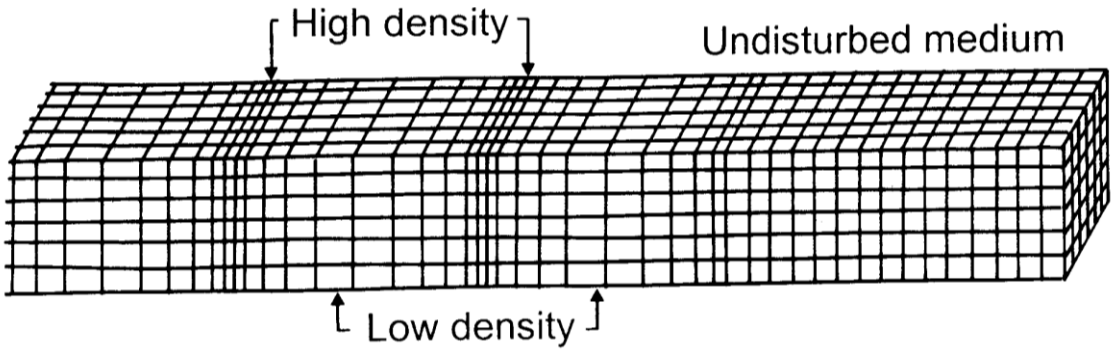

Figure 4.1: P-wave propagation (Landstreet 2009).

S-waves are on the other hand transverse waves. The meaning of shear deformation is that the particles are deforming in a direction perpendicular to the direction of propagation. The propagation of a S-wave is illustrated in Figure 4.2. Liquids have no shear resistance which makes it impossible for shear waves to propagate in them (Dahlin et al. 2001). That is a noteworthy fact considering the high water content in peat.

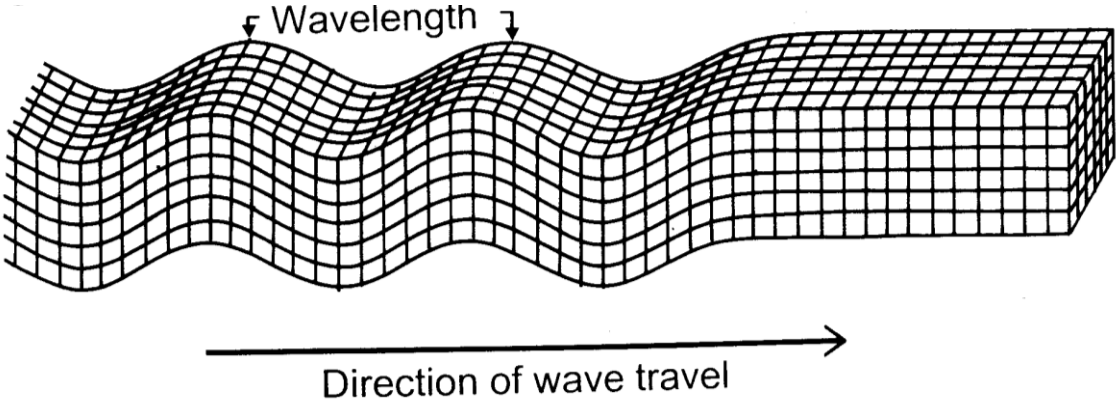

Figure 4.2: S-wave propagation (Landstreet 2009).

The P-wave velocity is related to the density, ρ, of the material and the oedometer modulus, M, whereas the S-wave velocity is related to density and shear modulus, G. This is expressed as:

$$V_p = \sqrt{M/\rho} \tag{4.1}$$

$$V_s = \sqrt{G/\rho} \tag{4.2}$$

The elastic constants are usually increasing rapidly with increasing depth resulting in an increase in velocity for the body waves. This is true although the density increases with depth since the elastic constants usually increases faster with depth. Assuming the P-wave velocity and S-wave velocity are known along with the density, Milsom & Eriksen (2011) state that the elastic constants can be calculated as follows:

$$(V_p/V_s)^2 = M/G = 2(1-\nu)/(1-2\nu) \tag{4.3}$$

i.e.

$$\nu = \left[2 - (V_p/V_s)^2\right]/2[1 - (V_p/V_s)^2] \tag{4.4}$$

and

$$M = E(1-\nu)/(1+\nu)(1-2\nu) \tag{4.5}$$

where ν is poisson´s ratio, E is Young´s modulus.

The small strain shear modulus $G_{\max}$ (kPa) can be calculated from the shear wave velocity and can be expressed as follows:

$$G_{\max} = \rho V_s^2 \tag{4.6}$$

This follows from Equation (4.2), note that G_{max} is used and refers to the shear modulus at a strain less than 0.0001 %. For this low strain, G behaves differently from the behavior at higher strains which is characterised by a decreasing G as the shear strain increases. Instead, for low strain rates, the shear modulus reaches a maximum value, G_{max} (Bui et al. 2010). $G_{\max}$ is mainly a function of void ratio, soil density and effective stress. It is also related to soil type, age, depositional environment, cementation and stress history (Hardin and Drnevich 1972).

4.2 Ground penetrating radar

It is of big significance to identify organic soils as the compressions are larger and the strength is poor compared to mineral soils (Huat et al. 2014). A method to identify the depth of a peat layer is Ground penetrating radar (GPR) from which a continuous image of the peat-mineral contact can be obtained (Proulx-McInnis et al. 2013). A GPR is nowadays often connected to a GPS and is used in design and risk assessment for infrastructure projects where peat soils are present (Long & Boylan 2012). In Figure 4.3 GPR is used at a peat bog.

Ground Penetrating Radar is used to detect changes in electrical properties, the method is based on electromagnetic waves that have frequencies ranging from 10 MHz to 4 GHz (Milsom & Eriksen 2011). It is a non-invasive method using a transmitting antenna for shallow subsurface investigation (Neal 2004; Comas et al. 2004).

Figure 4.3: GPR used in field work at a peat bog (Trafford & Long 2016).

The transmission velocities are important for interpretation. The velocity is almost independent of frequency for many materials for frequencies higher than 1 MHz. The relative magnetic permeability, μ, is usually assumed to be unity. It is therefore only changes in conductivity and relative electric permittivity that cause the reflection, dispersion and attenuation of the signals. These are usually assumed to be scalar quantities and do not depend on the direction of the radiating field.

Some of the GPR signal will be reflected if it reaches a discontinuity in magnetic permeability, electrical conductivity or dielectric permittivity. More will be reflected if the target is larger, it is also affected by the angle of incidence and the amplitude reflection coefficient for normal incidence. The reflection coefficient is mainly dependent on variations in water content for most materials.

The result is affected by the surface smoothness where rough surfaces drain energy resulting in reduced amplitude in reflections. Ideally, there is a smooth surface where the signal is mirrored where the angles of incidence and reflection match. At least 1 % of the signal should be reflected in order to obtain an adequate result. There is also an effect of attenuation due to the currents created from the radar waves. Energy from the waves are lost as heat from the currents eventually resulting in non-detectable wave amplitudes (Milsom & Eriksen 2011).

4.3 Relationship between shear wave velocity and shear resistance

Useful relationships have been found between shear wave velocity and shear strength, s_u, for clay which can be used to evaluate soil properties from V_s values (L´Heureux & Long 2017). According to L´Heureux & Long (2016) the relationship is reasonable since both V_s and s_u depend on the same variables. The authors found a relationship for Norwegian clay:

$$s_{u,DSS} = 0.02V_s^{1.45} \tag{4.7}$$

The regression coefficient is 0.91 and the plot of the individual data points are shown in Figure 4.4.

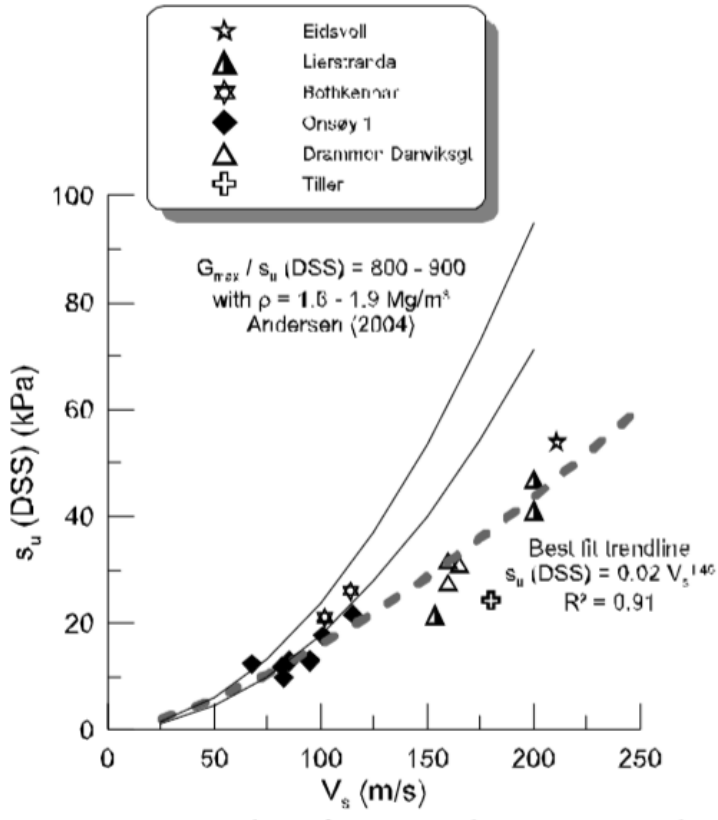

Figure 4.4: Plot of shear wave velocity against undrained shear strength for Norwegian clay. Graph from L´Heureux & Long (2016).

The shear strength was evaluated from direct simple shear tests (DSS). That method was also used by Trafford (2017) where the relationship between V_s and undrained shear strength was investigated for peat. The results are shown in Figure 4.5.

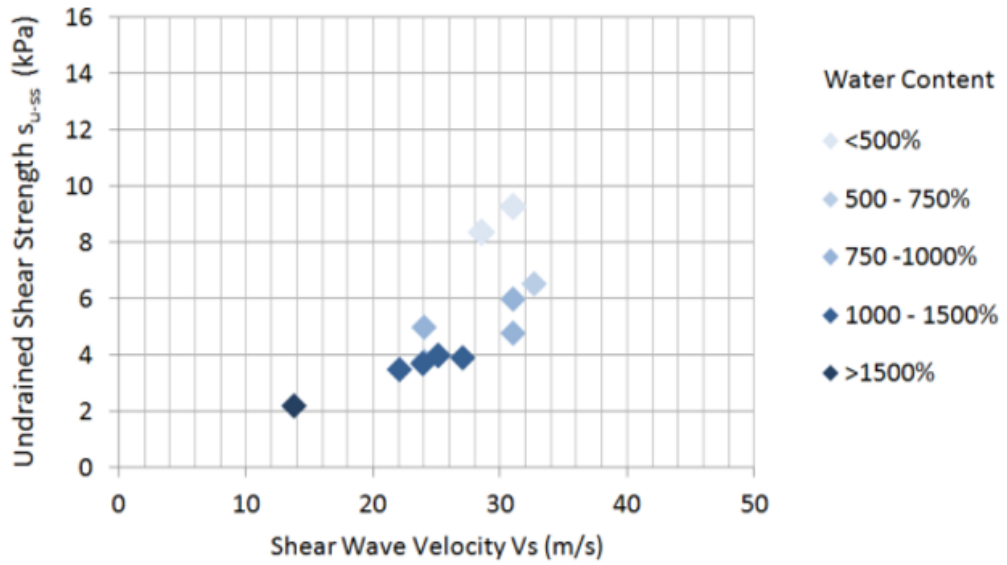

Figure 4.5: Plot of shear wave velocity against undrained shear strength for peat. Graph from Trafford (2017).

A relationship can be observed from the plot, with increasing scatter of s_u as V_s increases. Trafford (2017) state the relationship as generally accepted since the controlling factor of both

V_S and s_u is the shear resistance and the consolidation stress. This relationship appears to be valid for peat according to the empirical work.

4.4 Relationship between shear wave velocity and consolidation parameters

L´Heureux & Long (2017) investigated the relationship between shear wave velocity and 1D compression parameters for Norwegian clay. A useful relationship was found for both M_0 and M_L with respective R^2 values of 0.78 and 0.80 for the trend lines. The relations were given as:

$$M_0 = 0.00010 V_s^{2.212} \tag{4.8}$$

and

$$M_L = 0.00000014 V_s^{3.26} \tag{4.9}$$

A relationship was also found for $\sigma´_c$ with an R^2 value of 0.80 shown in Figure 4.6. It was expressed as:

$$\sigma´_c = 0.00769 V_s^{2.009} \tag{4.10}$$

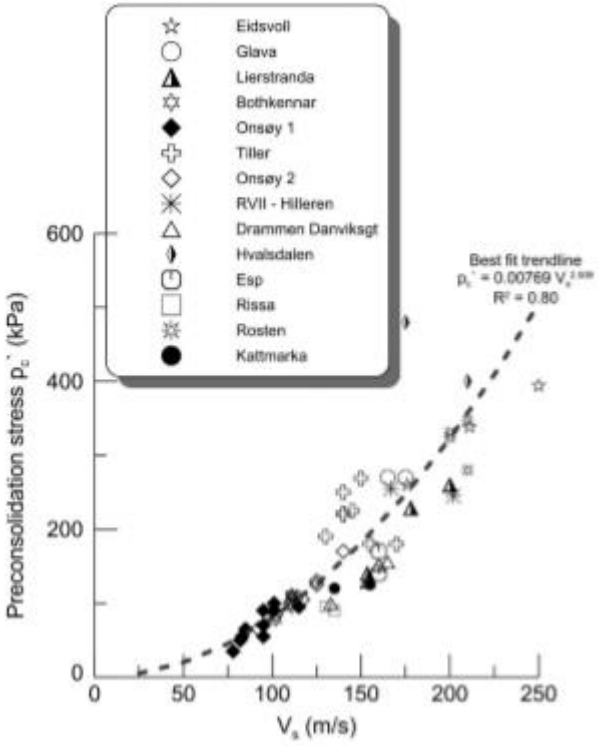

Figure 4.6: Plot of shear wave velocity against preconsolidation stress for Norwegian clay. Graph from L´Heureux & Long (2017).

It has been showed in Hardin & Richart (1963) study that V_s is a function of void ratio and the current state of stress. The function was proposed as:

$$V_s = (m_1 - m_2 e)(p´)^{0.25} \tag{4.11}$$

where e is the void ratio, $p´$ is the effective mean normal stress and m_1, m_2 are material constants.

Since V_s depends on the void ratio and the current effective stress it is plausible to evaluate the current state of the soil before loading (Lipiński et al. 2017). L´Heureux & Long (2017) showed this for compression parameters of Norwegian clay. There are no studies made on peat in this area but the relation found for clay suggest that a relation can be found for peat as well.

5 Field work

Field data is available from three different sites in Sweden:

- Ageröds mosse
- Färgelanda
- Mullsjö

The respective coordinates are presented in Table 5.1. The coordinate system is SWEREF 99 TM.

Table 5.1: Coordinates of the field sites.

Field site	Coordinates
Ageröds mosse	6199679, 401919
Färgelanda	6506629, 324507
Mullsjö SGI1	6414250, 439212
Mullsjö SGI2	6414198, 439194

Shear wave velocity measurements were performed on each site using Down hole method. In order to characterise the peat according to von Post scale of humification peat was extracted by a Russian sampler. Samples for water content measurements was also collected every 0.1 meter from the extracted soil.

5.1 Field sites

Field work was performed in Ageröds mosse which is a bog located in Höör Municipality. The majority of the block samples tested in this work was recovered from this site. Similar field investigations were performed in Färgelanda and Mullsjö.

5.1.1 Ageröds mosse

The field site at Ageröds mosse has earlier been subject for archaeological excavations which makes an impact on the site today. The depth of the peat is around 3.4 meters at the borehole. The location and a photo of the site is shown in Figure 5.1 and Figure 5.2.

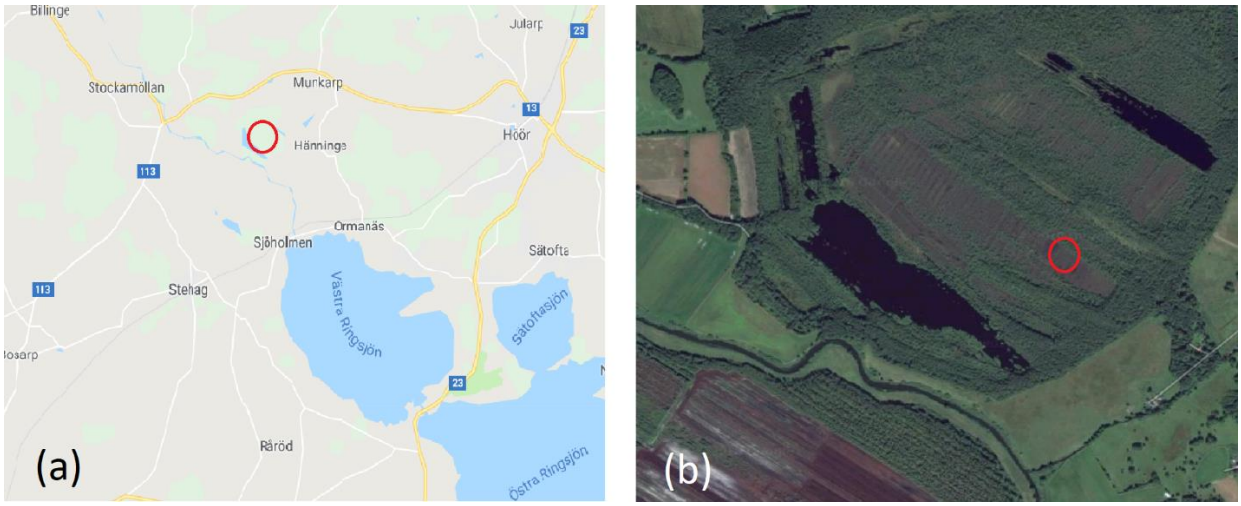

Figure 5.1: (a) Location on map, (b) Location on aerial view (Google Maps 2018).

Figure 5.2: Photo of the lightly forested site.

At a shallow depth the humification is around 4.5 to 6 on the Von post scale of humification. The peat is characterised as brown with low fibre content. For 0.4 meters to 0.7 meters the decomposition is small, see Figure 5.3. That implies high fibrous content which also is the case for fine fibres. There is a low content of coarse fibres and no wood and shrubs. It is a dark brown highly fibrous peat at this section. Further down the humification increases, between 0.9 to 1.3 meters the peat is brown with low fibre content. At 2.1 meters and below there is an involvement of timber fragments as can be seen in Figure 5.4. An increase of coarse fibres is also observed. The humification is generally 4-5 for the peat column except for the low fibrous section between 0.9 to 1.9 meters.

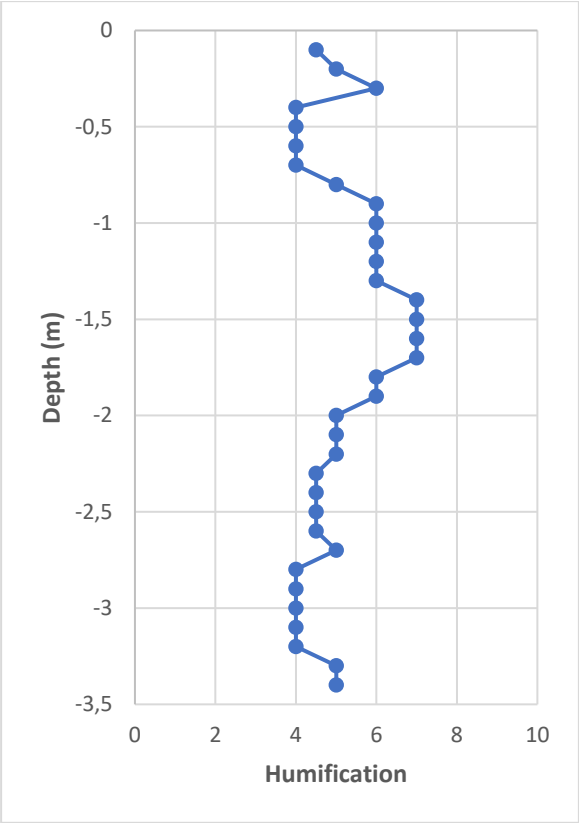

Figure 5.3: The variation of humification with depth for Ageröds mosse.

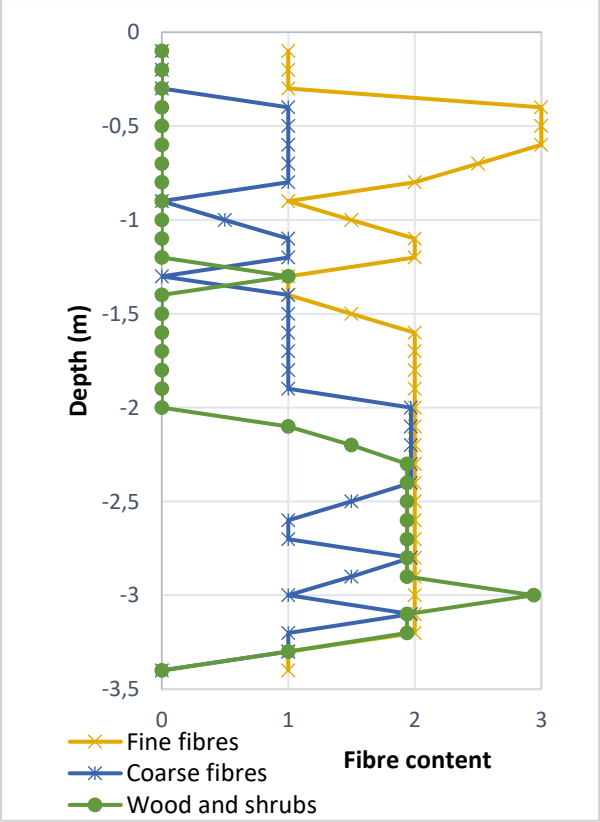

Figure 5.4: Content of fine fibres, coarse fibres and wood and shrubs in Ageröds mosse.

5.1.2 Färgelanda

The Färgelanda site was located adjacent to road 2081 in Västra Götaland County, where a vertical shear wave profile was obtained. The location is shown in Figure 5.5. One block sample was excavated in order to do CRS-tests. The peat depth at the site was around 5.7 meters.

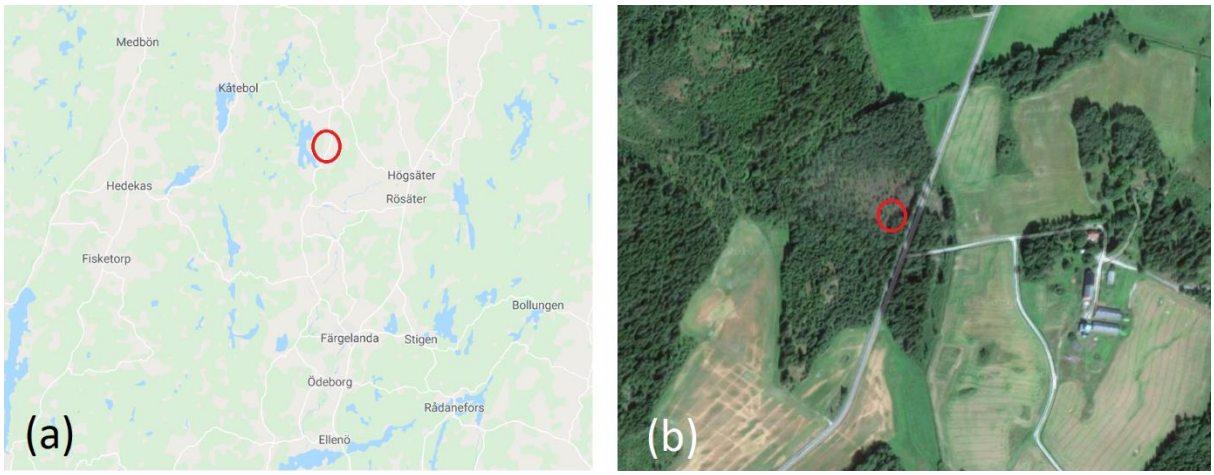

Figure 5.5: (a) Location on map, (b) Location on aerial view (Google Maps 2018).

The humification in Färgelanda is increasing with depth as is shown in Figure 5.6. This is the typical case as peat at a deeper level has had more time to decompose. The humification is spanning from 3 at shallow depth to 7 at the deepest level. The content of fine fibres is high and steady between 2 and 3 until it decreases at around 3.1 meters, see Figure 5.7. There is generally a low content of coarse fibres, from 2.3 – 3.3 meters there is no content of coarse fibres. Likewise, there is no wood and shrubs until the depth of 2.3 meters.

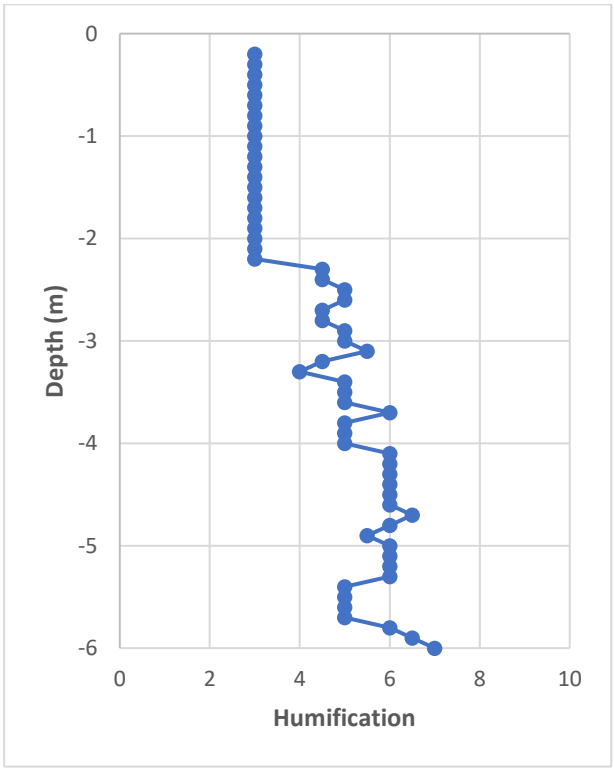

Figure 5.6: The variation of humification with depth for Färgelanda.

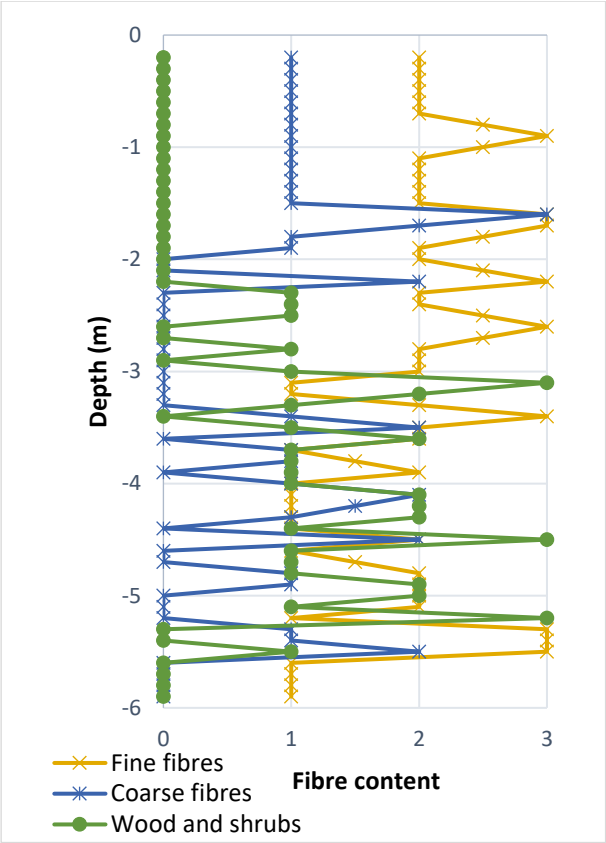

Figure 5.7: Content of fine fibres, coarse fibres and wood and shrubs in Färgelanda.

5.1.3 Mullsjö

The testing was performed adjacent to an embankment near the town Mullsjö. The site will in the future be subjected to further investigations by SGI. Two vertical shear wave profiles were obtained at different spots, SGI1 and SGI2, where the coordinates are shown in Table 5.1. SGI1 was located 10 meters from the toe of the embankment and SGI2 was located 20 meters from the toe of the embankment. The embankment cannot be seen from the aerial view in Figure 5.8. One block sample was excavated, at SGI1, in order to do CRS-tests. The peat thickness varied from 2.0 meters at SGI2 to 3.6 meters at SGI1.

Figure 5.8: (a) Location on map, (b) Location on aerial view (Google Maps 2018).

5.1.3.1 SGI1

An orange/brown spongy sphagnum layer was observed at the top 2.0 meters of the peat profile. Figure 5.9 shows a low level of decomposition for this upper part of the profile. There is a high content of fine fibres without any mixture of thicker fibres, see Figure 5.10. A transition is then observed to brown fibrous peat before a layer of grey organic clay. The fibrous peat layer was 1.4 meters deep. The humification is higher there compared to the sphagnum layer and there is an involvement of course fibres and timber fragments.

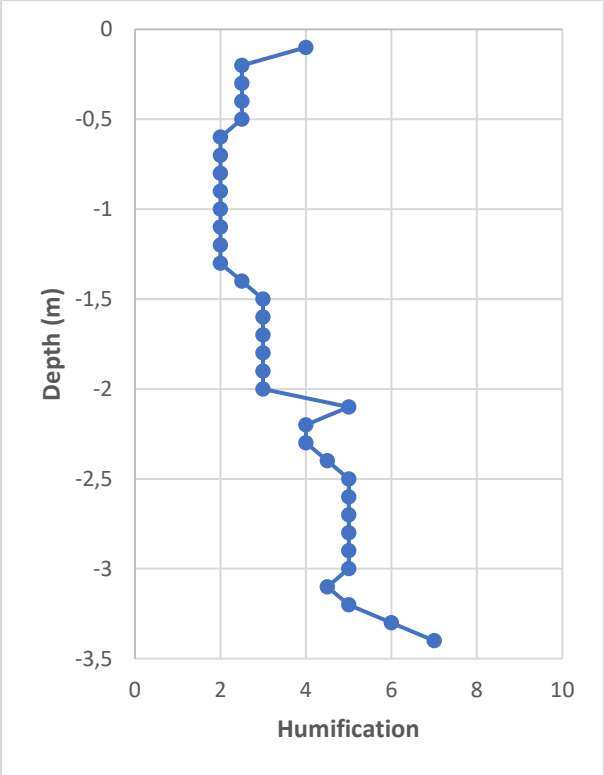

Figure 5.9: The variation of humification with depth for SGI1.

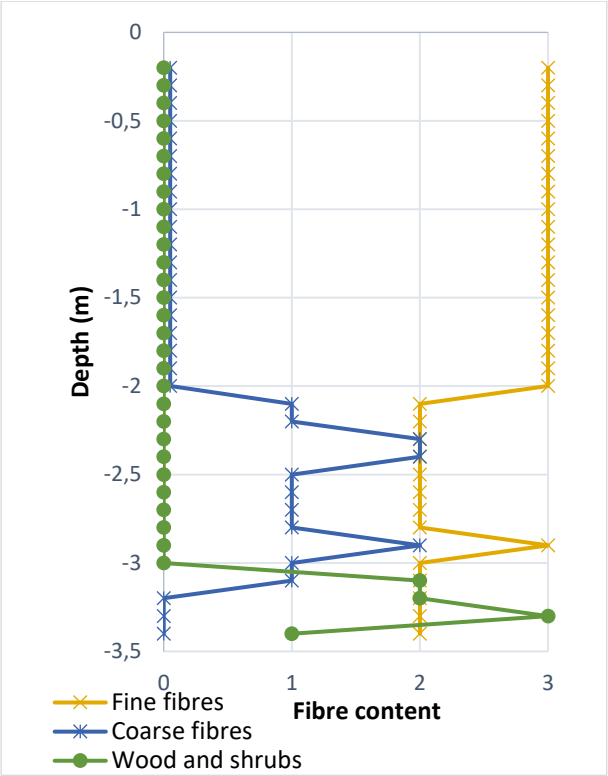

Figure 5.10: Content of fine fibres, coarse fibres and wood and shrubs in SGI1.

5.1.3.2 SGI2

The spongy sphagnum layer observed in SGI1 is shallower in SGI2, 1.6 meters. The following fibrous layer is 0.4 meters. Because of the stiff fibrous layer in SGI2 it was not possible to log the peat for the full profile or evaluate the water content. The samples recovered was not regarded as representative to the in situ soil. The scattered data of humification and fibre content is shown in Figure 5.11 and 5.12 respectively.

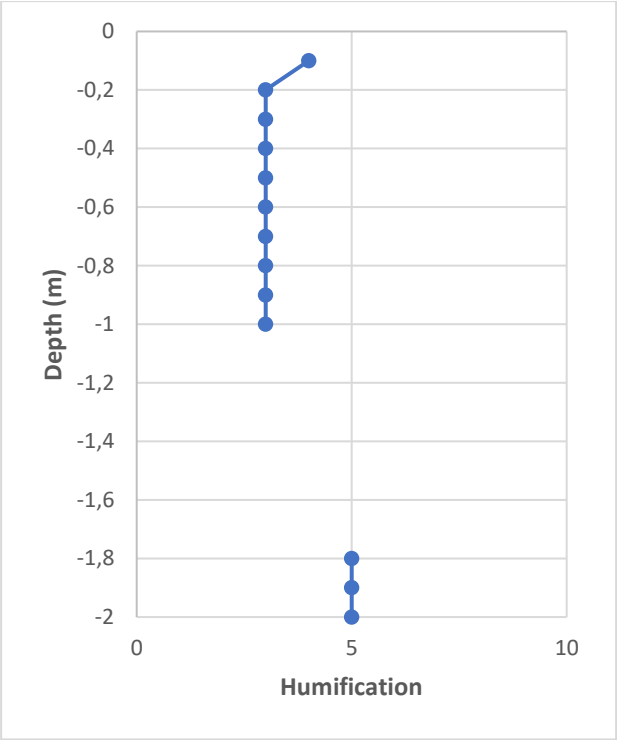

Figure 5.11: The variation of humification with depth for SGI2.

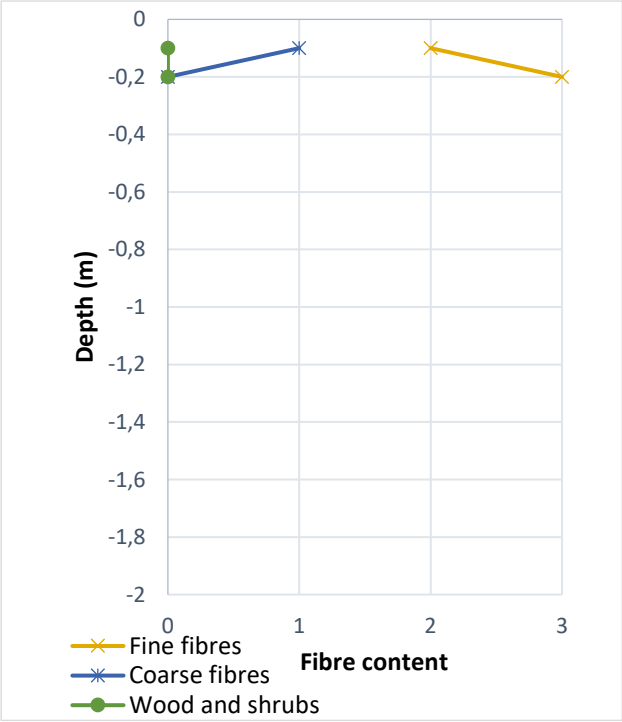

Figure 5.12: Content of fine fibres, coarse fibres and wood and shrubs in SGI2.

6 Results

6.1 Shear wave profiles

6.1.1 Ageröds Mosse

The plot in Figure 6.1 shows a high velocity section between 2.1 meters to 3.0 meters at around 30 m/s. It corresponds with the section of fibrous peat. There is also a tendency of higher velocity at the fibrous layer 0.4 meters to 0.7 meters. There is not an obvious increase of V_s with depth.

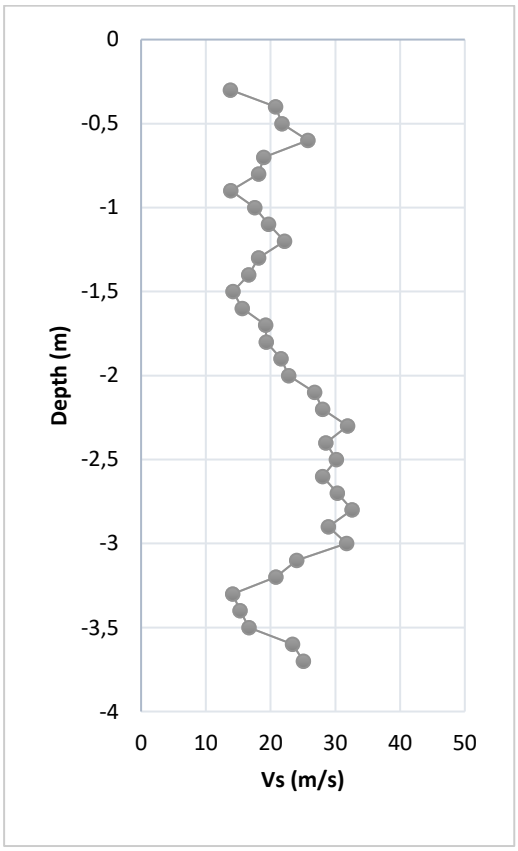

Figure 6.1: The variation of shear wave velocity with depth for Ageröds mosse.

The water content for the whole peat column varies from around 650 % to 1000 %. It is not particularly high for peat. For the fibrous section from 1.8 meters to 3.0 meters the water content is almost constant at around 800 %. See Figure 6.2.

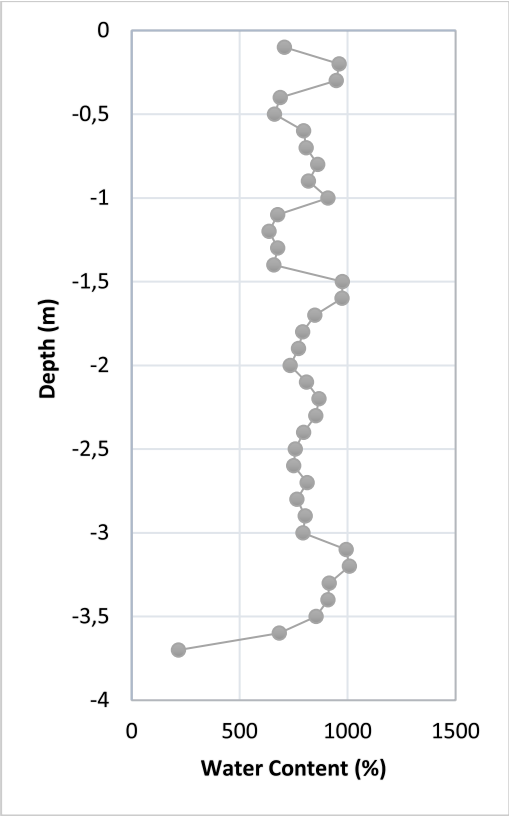

Figure 6.2: The variation of water content with depth for Ageröds mosse.

The combined plot in Figure 6.3 between water content and shear wave velocity shows that V_s increases as the water content decreases. This is not the case from 2.2 meter to 3.0 meter where the relationship is the opposite or harder to determine.

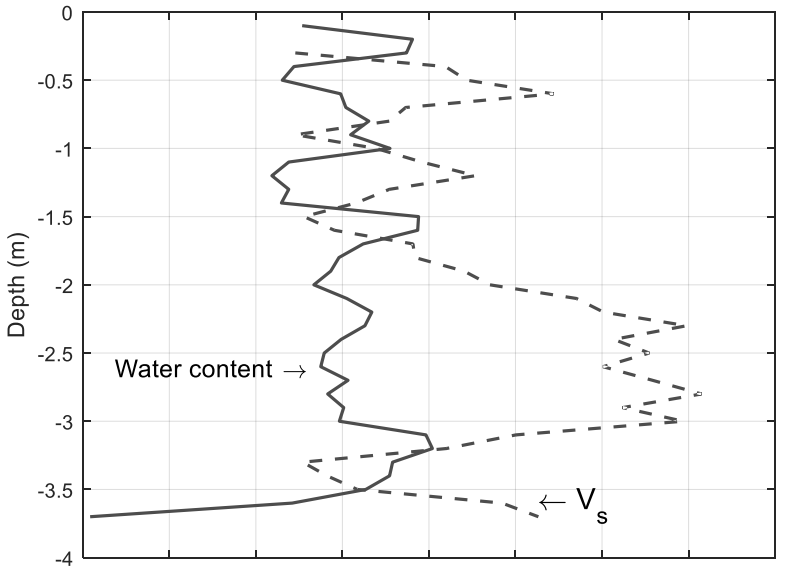

Figure 6.3: Plot of V_s compared to water content for Ageröds Mosse.

6.1.2 Färgelanda

The V_s profile in Färgelanda is shown in Figure 6.4. There is a tendency of increasing V_s with depth. It is ranging from 13.8 m/s to 34.2 m/s with the highest velocities in fibrous layers containing timber fragments.

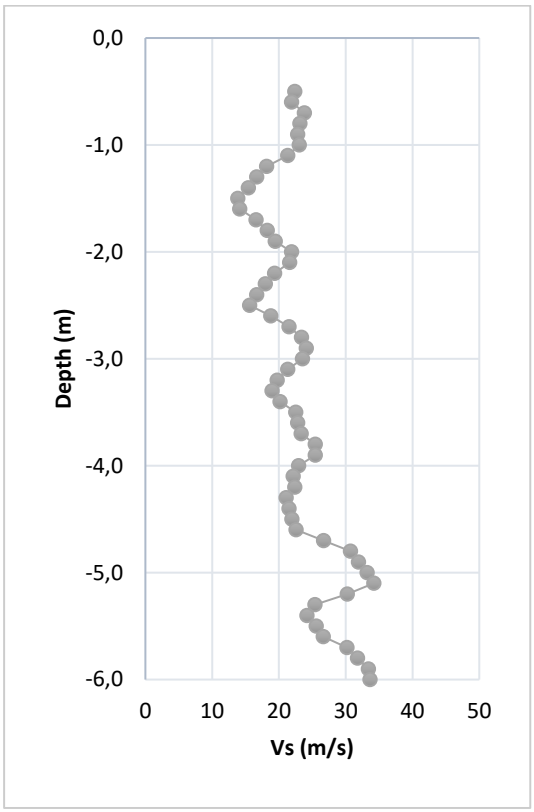

Figure 6.4: The variation of shear wave velocity with depth for Färgelanda.

The water content varies from 345 % to 1806 %. The highest value is a single high value surrounded with values around 800 % making it plausible it is invalid. Other than that there is a high water content between 0.9 and 2.1 meters for the section with orange/brown fibrous peat as can be seen in Figure 6.5.

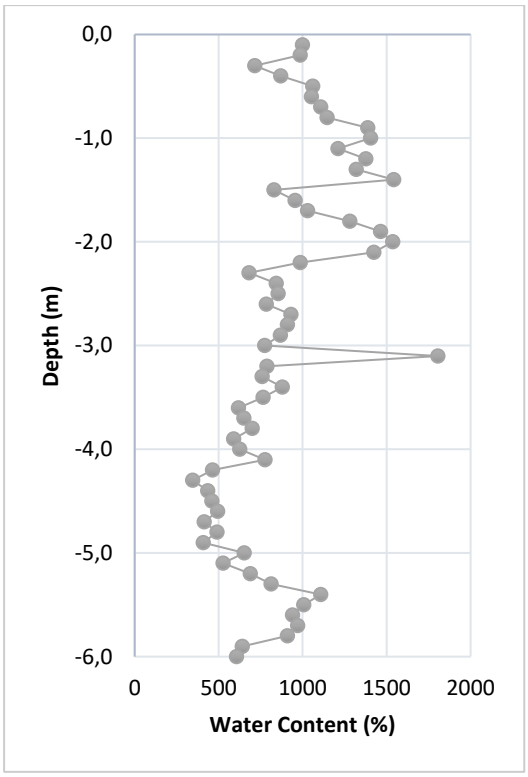

Figure 6.5: The variation of water content with depth for Färgelanda.

A plot of water content against V_s from the site at Färgelanda is shown in Figure 6.6. For the upper 2.2 meters the water content and V_s are correlating. The opposite is observed between 3.2 to 6 meters.

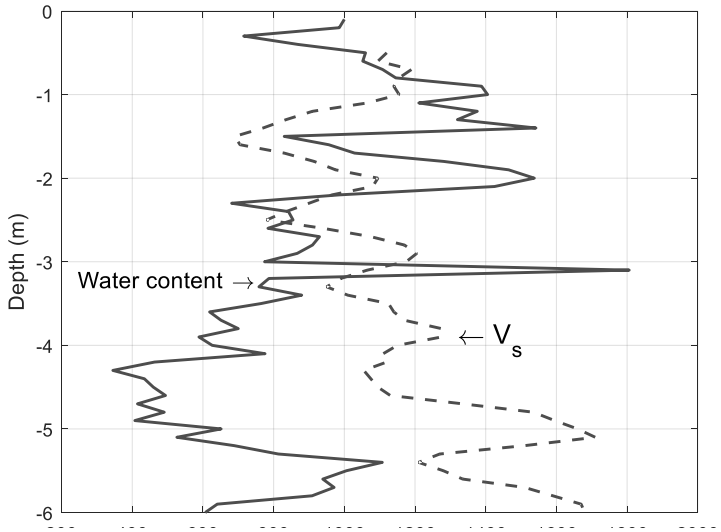

Figure 6.6: Plot of V_s compared to water content for Färgelanda.

6.1.3 Mullsjö

6.1.3.1 SGI1

The shear wave velocity in the peat column at SGI1, shown in Figure 6.7, varies from 11.2 m/s to 22.6 m/s. The highest values are almost linearly displayed between 3.0 and 3.6 meters, in the fibrous layer. There is a big variation of V_s in the sphagnum layer, which is located in the upper two meters.

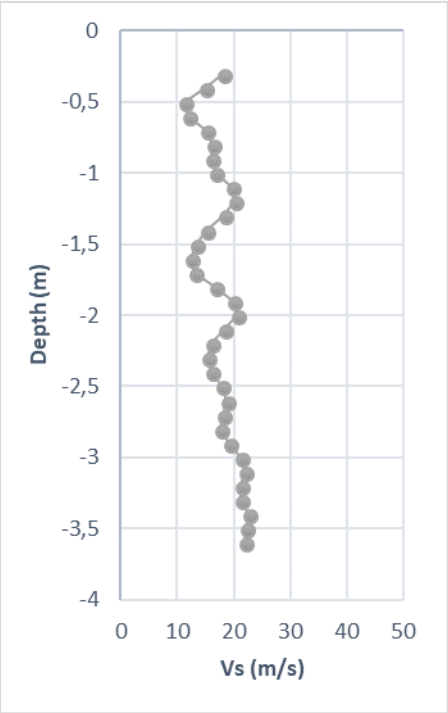

Figure 6.7: The variation of shear wave velocity with depth for SGI1.

The water content at SGI1 varied between 650 % to 2200 %, see Figure 6.8. The upper meter of the sphagnum layer has an average water content of 1150 %. Further down the water content increases, from 1.1 meters to 1.9 meters there is an average of 1650 %. At 2.0 meters the water content decreases to 1185 %, likely due to the mixture of more fibrous peat. The transition to fen peat results in an average water content of 900 %.

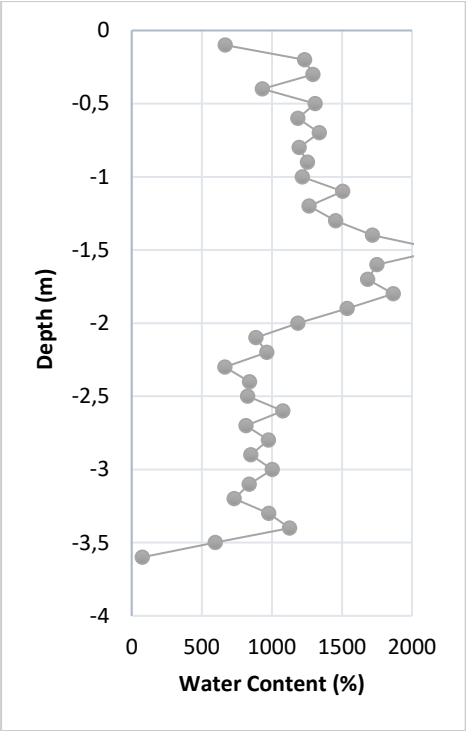

Figure 6.8: The variation of water content with depth for SGI1.

The combined plot of V_S and water content against the depth for SGI1 is shown in Figure 6.9. There is not an obvious relationship, however, for the upper 2.0 meters reverse correlation is indicated.

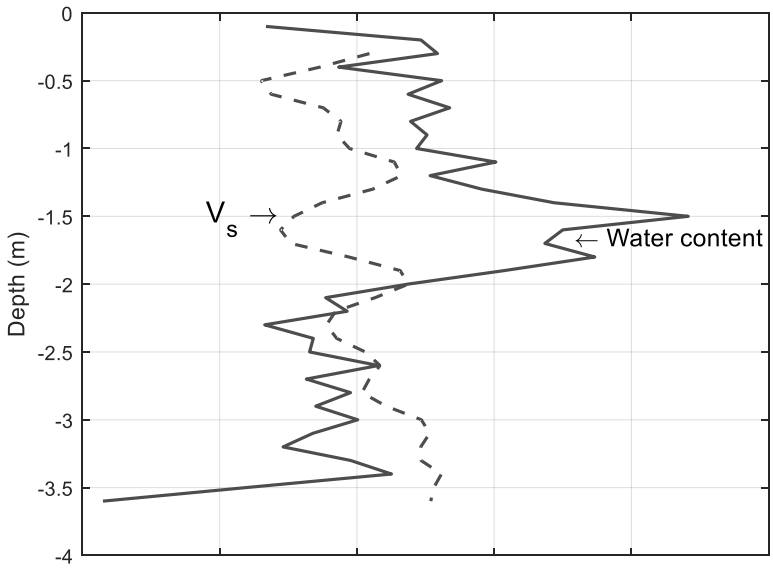

Figure 6.9: Plot of V_s compared to water content for SGI1.

6.1.3.2 SGI2

The shear wave velocity is generally increasing with depth in SGI2, as can be seen in Figure 6.10. The largest increase at 1.6 meters is occurring as there is a transition from a spongy sphagnum layer to fibrous peat.

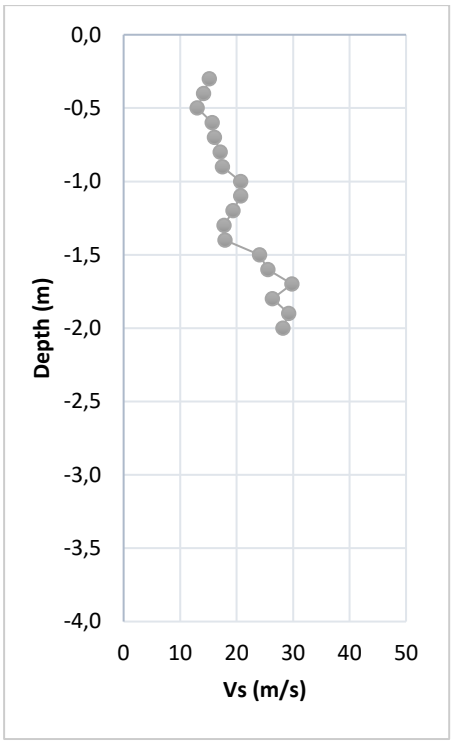

Figure 6.10: The variation of shear wave velocity with depth for SGI2.

The water content data is not complete for SGI2 because of the disturbance by the stiff fibrous layer. The obtained data, shown in Figure 6.11, is displaying a large variation of the water content.

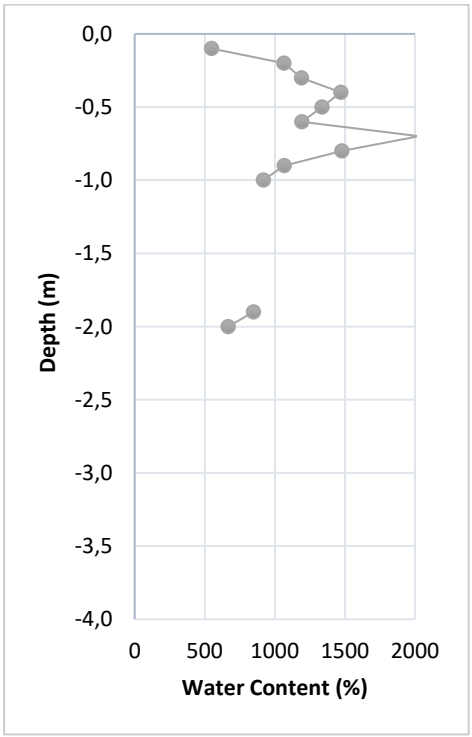

Figure 6.11: The variation of water content with depth for SGI2.

The combination plot between V_s and water content is shown in Figure 6.12. Because of the missing water content data, it is not possible to make any conclusions about the relation at SGI2.

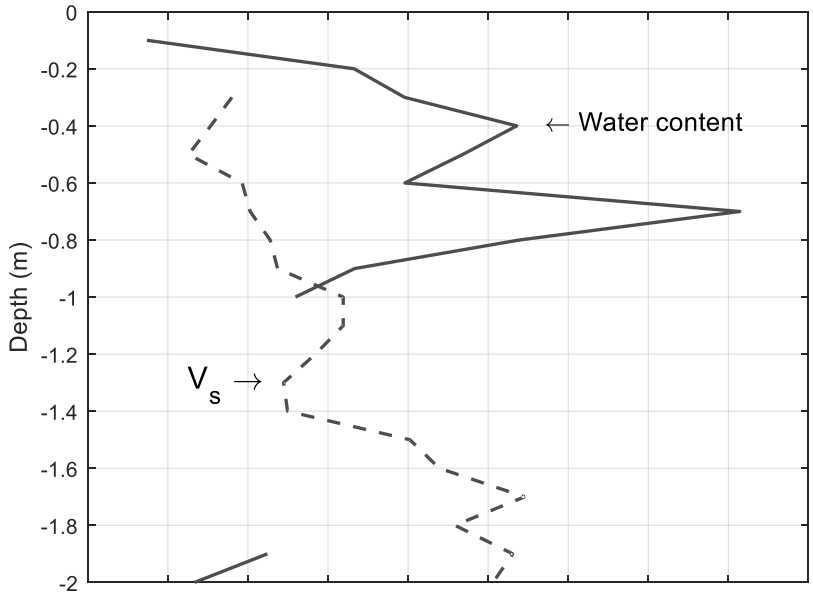

Figure 6.12: Plot of V_s compared to water content for SGI2.

6.2 CRS-testing

During CRS-testing a number of different rates were tested before choosing 0.00938 mm/min. For initial tests with higher rates the pore water pressure was increasing fast, therefore a slower rate was eventually chosen. The samples tested in the oedometer was 15 mm thick with a diameter of 77 mm. That results in a rate of 3.75 % per hour.

The setup procedure started with saturating the sample and getting any air out of the system, the oedometer used is shown in Figure 6.13. Air stuck in the tube connecting the oedometer with the pump had to be pumped out as well. The pump pressure was then set to 50 kPa. At that point the steel rod was put into place, connecting the load cell and the oedometer. This was cautiously done using a spirit level to make sure it was kept vertical. The displacement transducer was then glued on and the test was ready to begin.

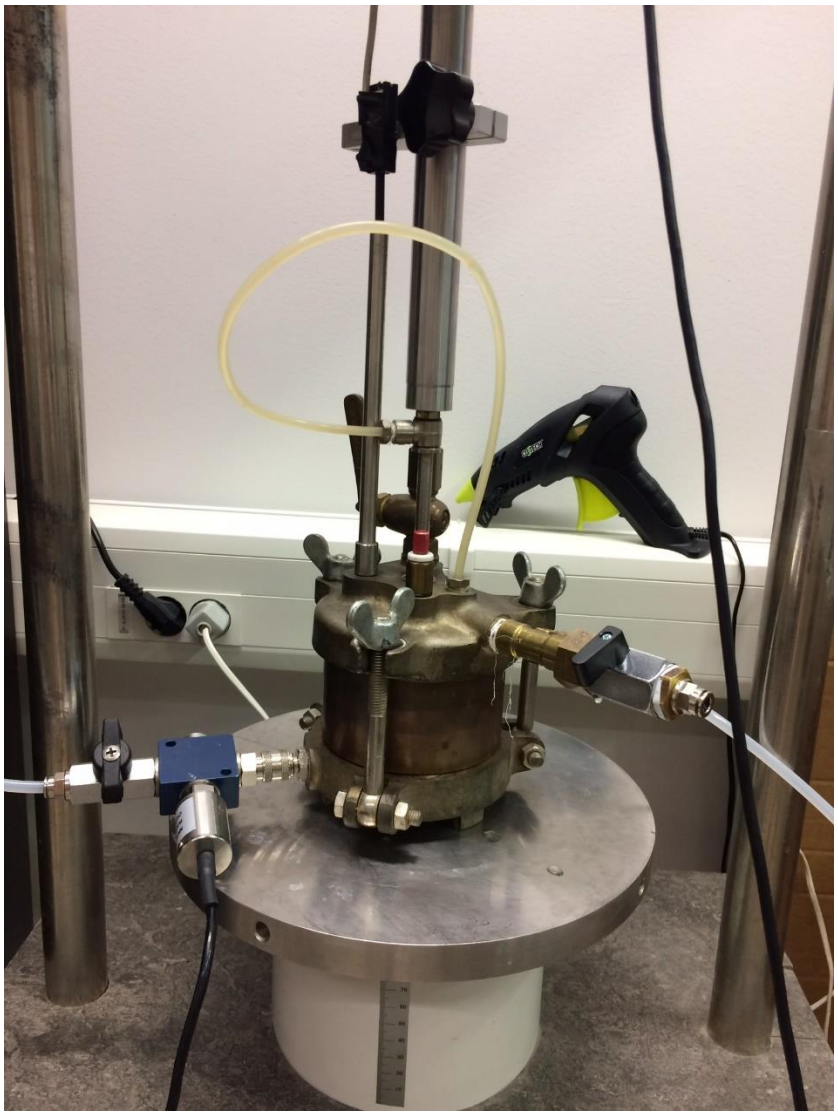

Figure 6.13: The oedometer used for CRS-tests.

It was not possible to press the oedometer without using a steel rod connecting the load cell and the device. This results in a small increase of the force which was taken into account in the calculations. The effective stress was calculated by using (3.2).

During testing the porous stones split up in three and four pieces. The force applied on them was too high as the peat was compressed to around 80-85 %. This is due to the rapid increase in the oedometer modulus as the stress exceeds σ'_L as can be seen in the plots 6.14 to 6.18. No plot of σ' against c_v are shown due to issues in obtaining comparable values to what can be expected.

6.2.1 Variation of M with increasing σ'_c.

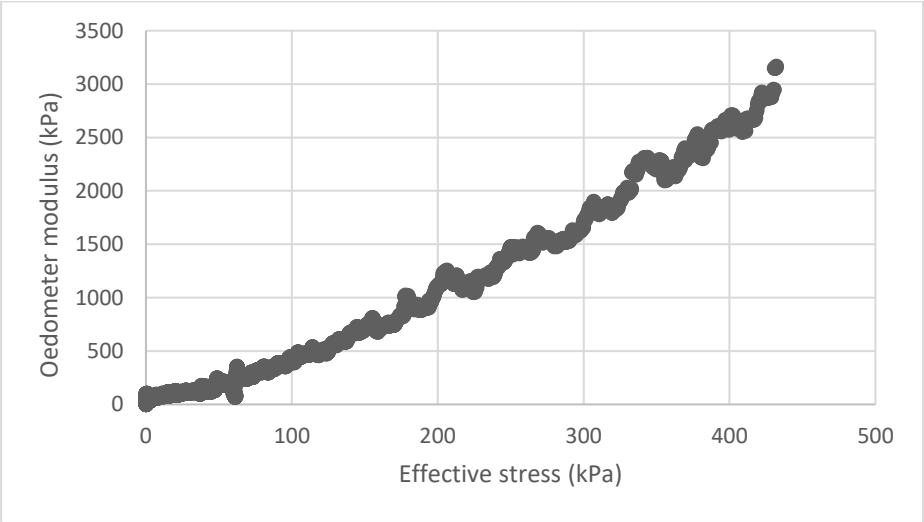

(a) Compression of sample 1 at depth 300 mm from Ageröds mosse.

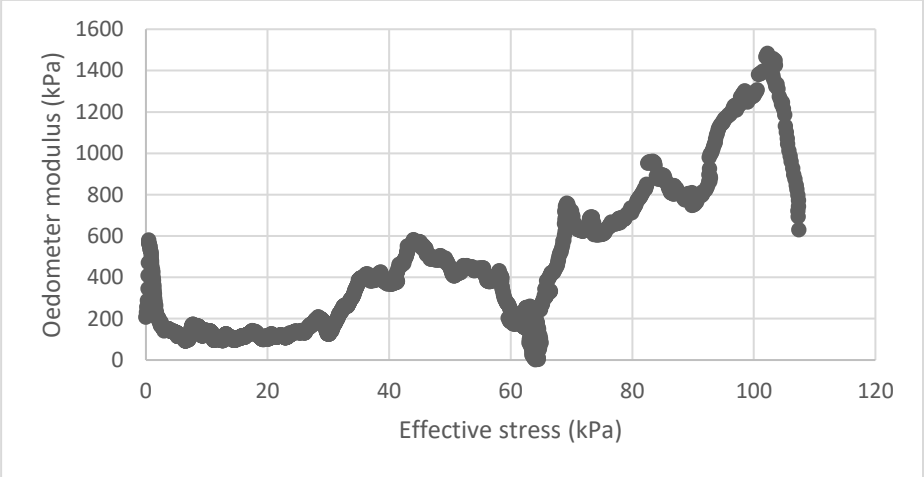

(b) Compression of sample 2 at depth 300 mm from Ageröds mosse.

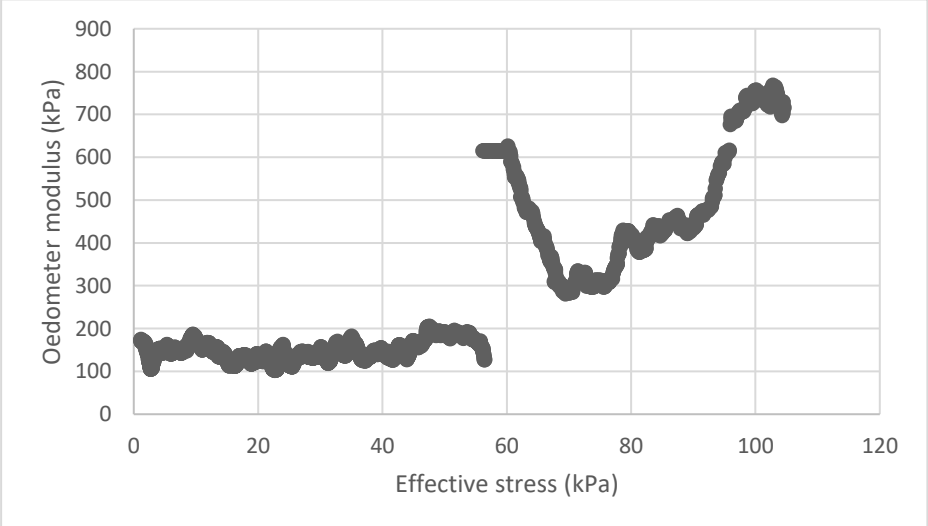

(c) Compression of sample 3 at depth 300 mm from Ageröds mosse.

Figure 6.14: Variation of the oedometer modulus with increasing effective stress.

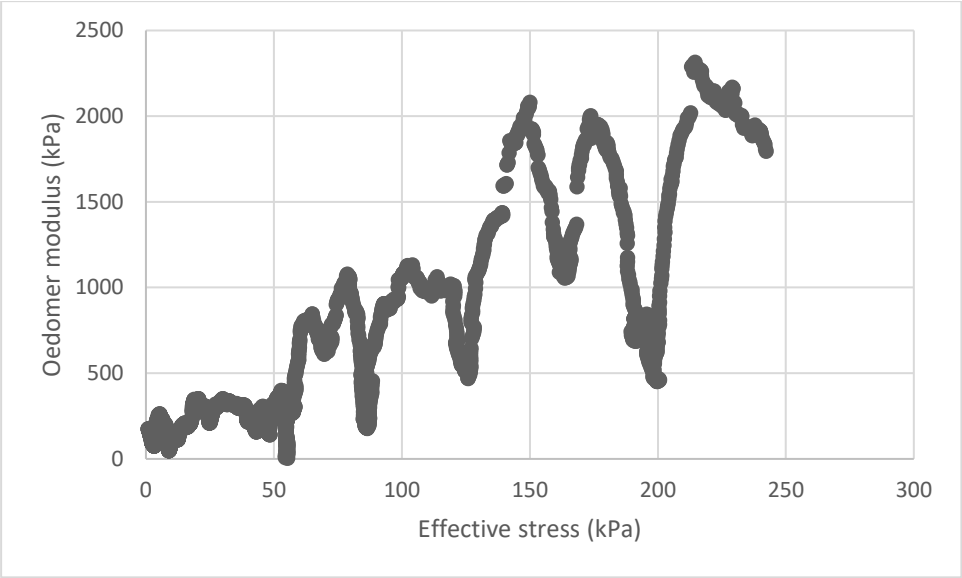

(a) Compression of the sample at depth 400 mm from Ageröds mosse.

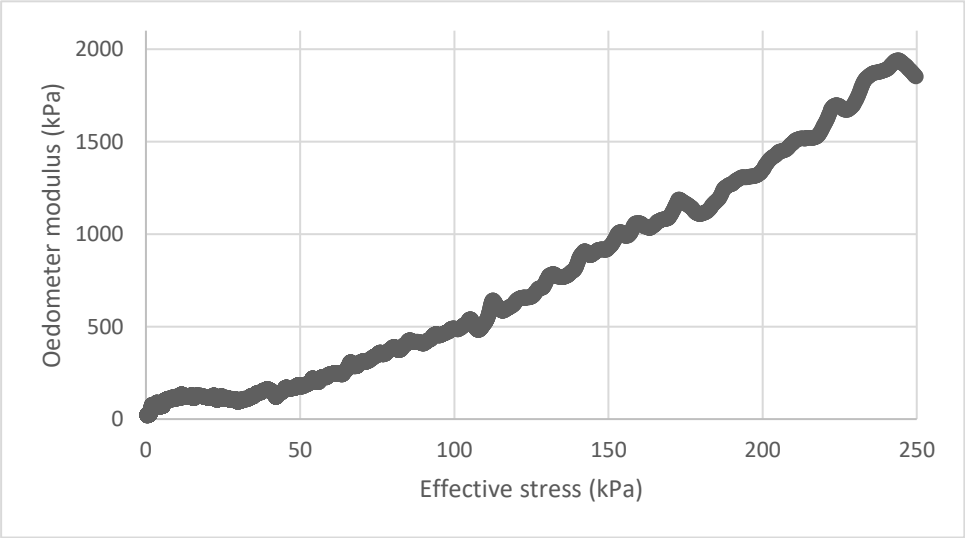

(b) Compression of sample 1 at depth 500 mm from Ageröds mosse.

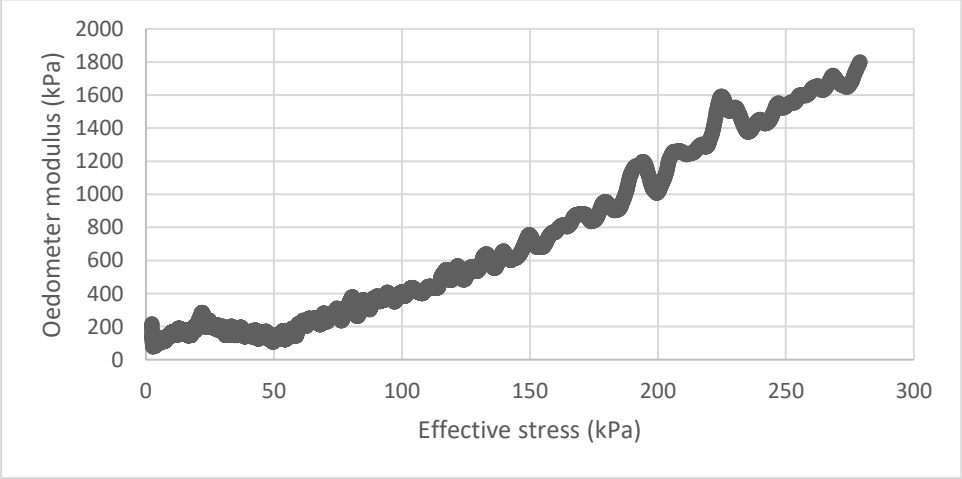

(c) Compression of sample 2 at depth 500 mm from Ageröds mosse.

Figure 6.15: Variation of the oedometer modulus with increasing effective stress.

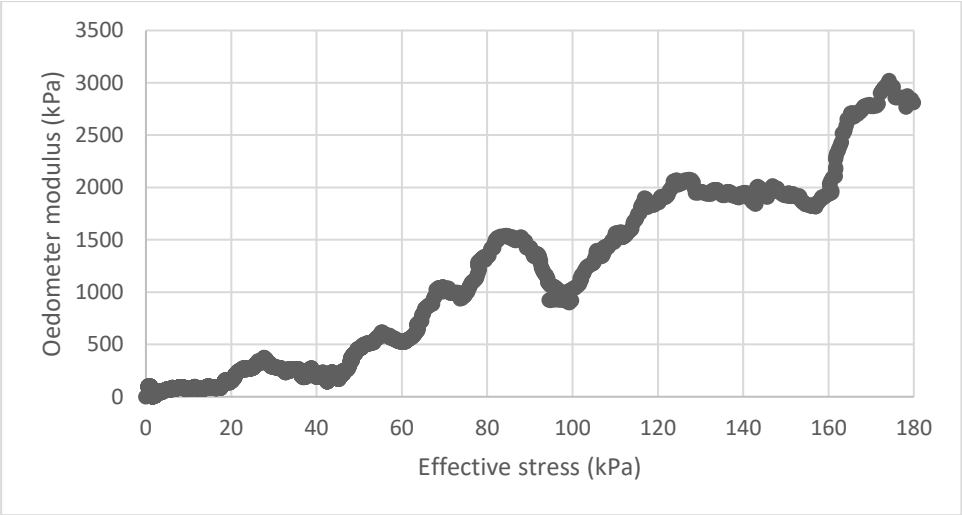

(a) Compression of the sample at depth 600 mm from Ageröds mosse.

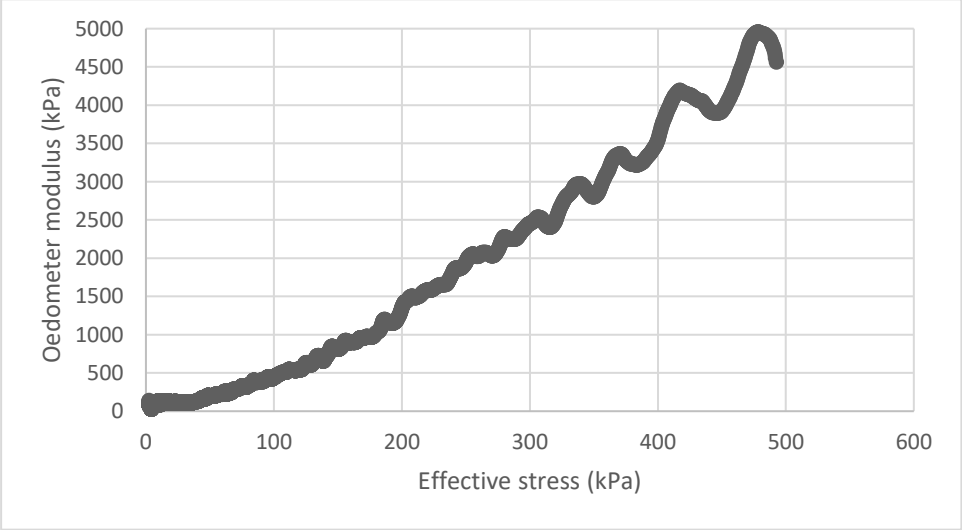

(b) Compression of sample 1 at depth 700 mm from Ageröds mosse.

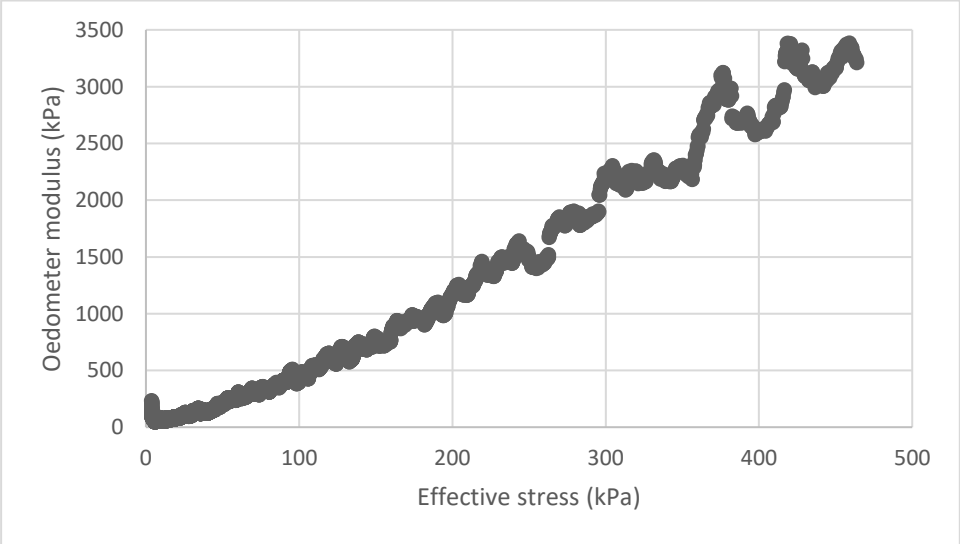

(c) Compression of sample 2 at depth 700 mm from Ageröds mosse.

Figure 6.16: Variation of the oedometer modulus with increasing effective stress.

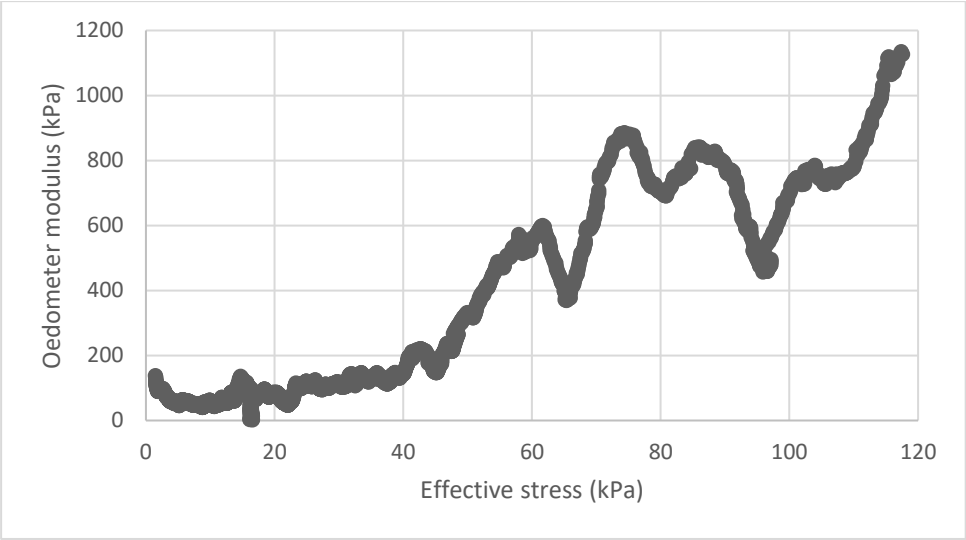

(a) Compression of sample 3 at depth 700 mm from Ageröds mosse.

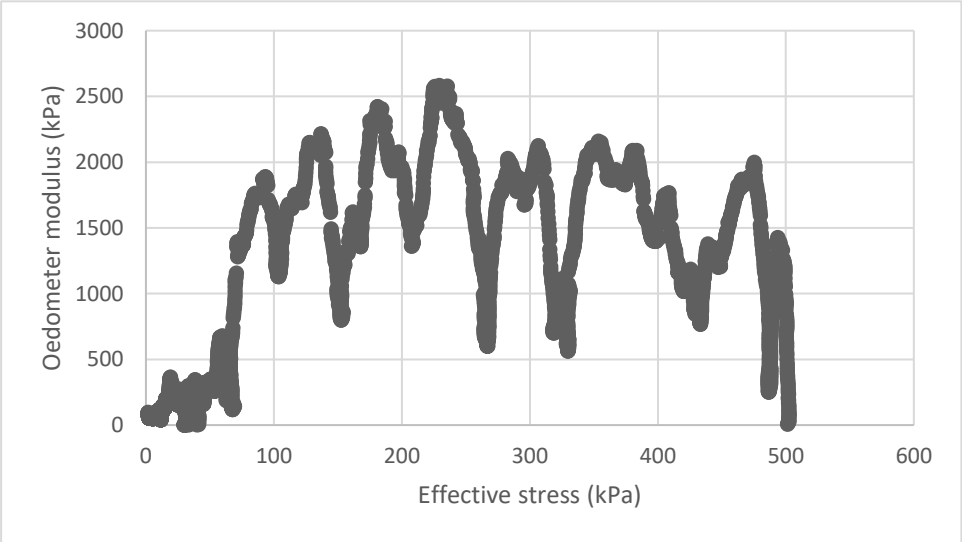

(b) Compression of the sample at depth 900 mm from Ageröds mosse.

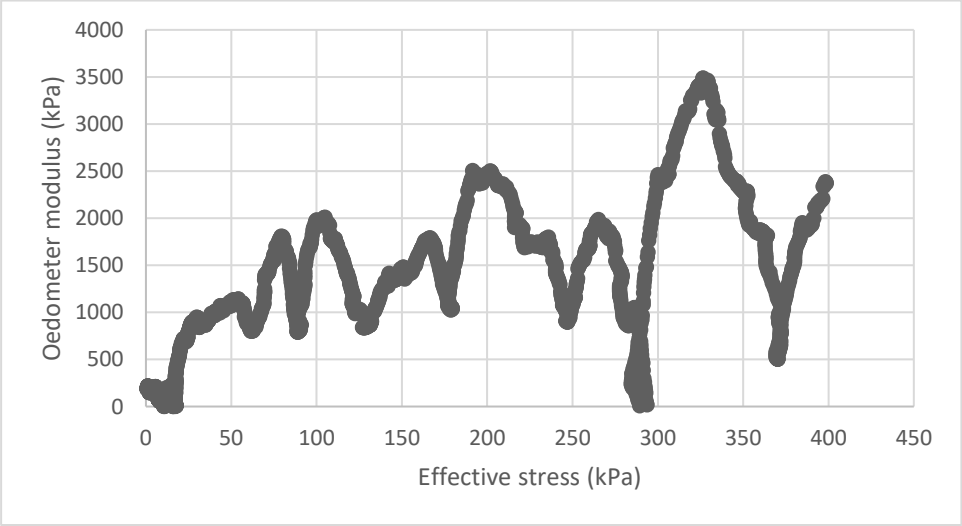

(c) Compression of the sample at depth 600 mm from Färgelanda.

Figure 6.17: Variation of the oedometer modulus with increasing effective stress.

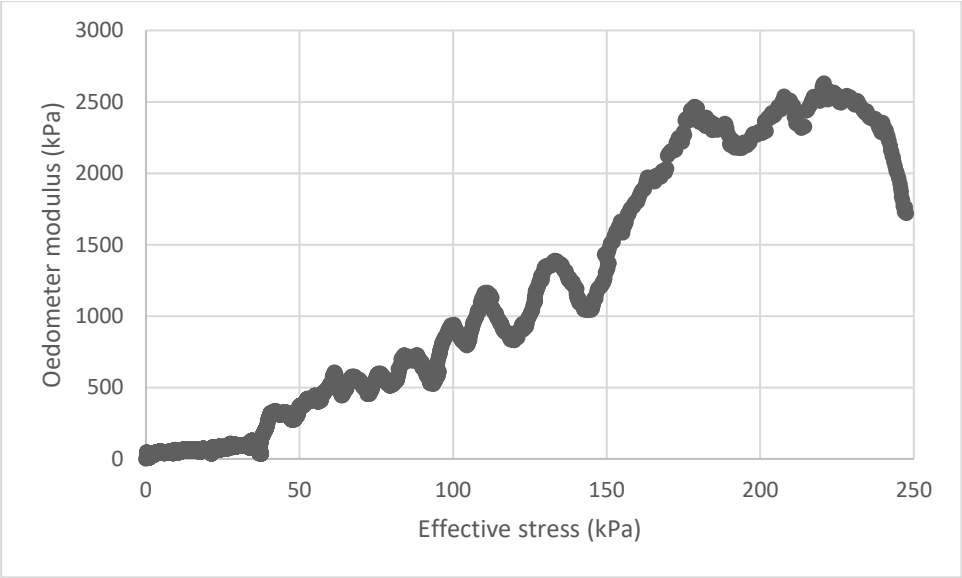

Figure 6.18: Compression of the sample at depth 600 mm from SGI1.

6.2.2 Comparison between V_s and consolidation parameters

From the 13 oedometer tests performed it has been possible to evaluate both M_L and m. It was not possible to evaluate σ'_c or M_0. A plot of V_s and the corresponding values of M_L is shown in Figure 6.19. There is a weak indication of increasing M_L with increasing V_s. The R^2 value is low at 0.1645 for a linear regression. There is a large variation of M_L, for instance the four M_L values corresponding to V_s =13.8 m/s ranges from 93.7 kPa to 180.3 kPa.

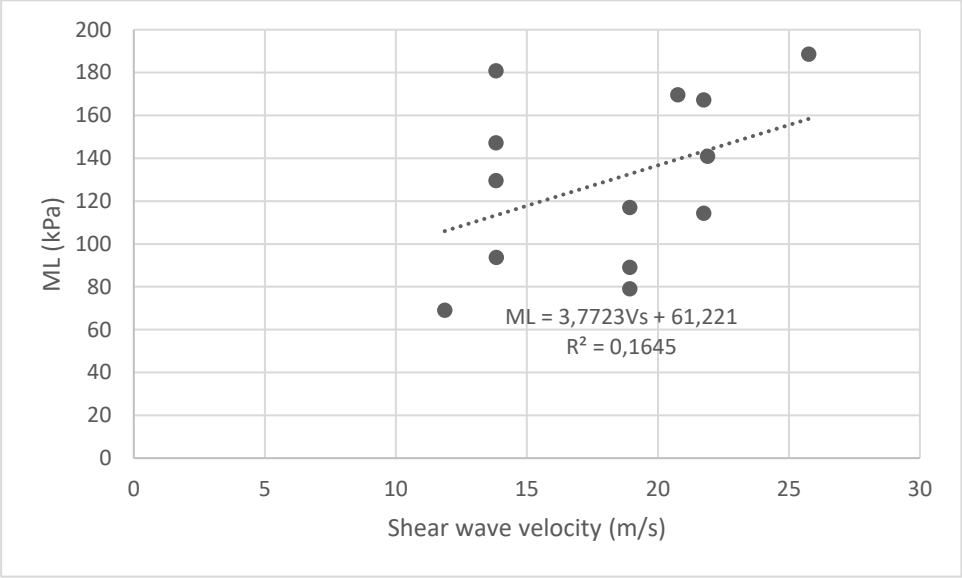

Figure 6.19: Plot of V_s against M_L based on the 13 tested samples.

Figure 6.20 shows the plot of V_s compared to m. There is no indication of a correlation based on the data.

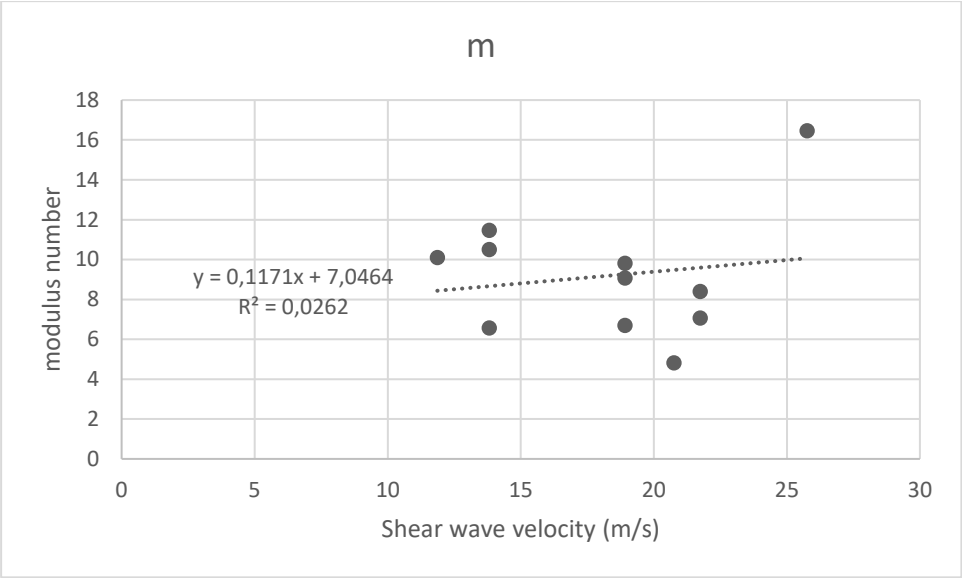

Figure 6.20: Plot of V_s against m based on the 13 tested samples.

The results from the tests where the porous stones are intact are summarised in Table 6.1. The data needs to be complemented to make any conclusion.

Table 6.1: Results of V_s with corresponding values of M_L and m.

V_s (m/s)	M_L (kPa)	m
13.82	129.5	6.6
21.75	114.3	8.4
21.75	167.2	7.1
18.92	117.0	9.1
18.92	89.0	6.7

7 Discussion and conclusions

The oedometer used in the test did not allow for a thicker sample than 15 mm. This is not optimal for peat because of its heterogeneous nature as it was discussed by Long & Boylan (2013). Ideally a sample that is thicker than 20 mm should be used. However, multiple tests have run at the same level when possible. Factors limiting this opportunity has been the size of the block sample and the time constraint. Unfortunately, it was not possible to evaluate σ'_c or M_0. There was indications of an initial higher oedometer modulus for a few tests, this was indistinct and it was hard to interpret with any certainty. Since the unit weight of peat is only slightly larger than that of water, σ'_c would be very low if the groundwater level is close to the surface. That is why it is harder to evaluate σ'_c in some peat compared to clay.

A large variation of M_L and m was found without any obvious correlation with V_s based on the limited data in this study. A weak indication of a relationship can be seen for M_L. For the samples tested in the oedometer from the same depth and site the variation was rather large. An example is that M_L varied from around 130 kPa to 180 kPa and m from 6.6 to 11.5 for samples at depth 300 mm in Ageröds mosse. It is unlikely the properties of the samples are as different as these numbers suggest, there are undoubtedly sources of errors during testing that explain some of the differences. The major one would be the shattered porous stones that affected several of the tests. Peat is however a heterogeneous material and some differences are to be expected.

Regarding the water content in this study a reverse relation with V_s was observed in most cases as expected. At times this was not apparent, even the opposite relation was seen at short sequences.

In Färgelanda and Mullsjö, V_s increased with depth. This was not observed in Ageröds mosse even though earlier work has shown that V_s is linked to the effective vertical stress. However, there are other parameters controlling V_s such as void ratio.

Since shear waves do not propagate in liquids, the high water content of peat does not affect the shear wave velocity. This is not the case for compressional waves. That makes the water content the dominating factor deciding the velocity of the compressional waves in peat. That is why shear waves where considered in this study while compressional waves were not. For this reason, Poisson´s ratio was not evaluated and used in this study.

An issue with the results is that the oedometer testing was performed five months after the sampling due to incomplete equipment. This could imply that the samples have lost some of the water and it is plausible that the properties of the peat have changed even though the samples were stored in a cold storage area at around 4°C. For example, the organic particle size could have changed from sampling to the oedometer testing. This was the case for peat investigated by Mofidpoor et al. (2009), who found that longer storage time results in smaller particles. The particle size was investigated for three different storage times, 1, 3 and 10 months for both upper layer fibric peat and decomposed peat in their study. Another issue with decrease in water content is that there were difficulties compressing the samples to 80-90 % as has been done in previous work. That in addition to the fairly low water content at Ageröds mosse subjected the porous stones in the oedometer for a large stress.

The steel rod connecting the load cell and the oedometer device had a tendency to displace laterally during a few of the tests when the force increased to around 1.5 kN. As that happened the force reduced to around 50 N making the rest of the test invalid. This happened during two tests despite cautious setup using a spirit level.

7.1 Proposed further research

There is a need of further work with obtaining and analysing data in order to make more certain statements about the relationship between V_s and consolidation parameters. This can be tested on peat with different characteristics, similar to this study. It can also be specified what type of peat is tested, e.g. sphagnum or fibrous peat. There is a possibility of finding stronger relationships when the peat type is specified. On the downside, the results may be harder to apply.

8 References

Bui, Man T., Clayton, C.R.I. & Priest, J.A. (2010). The universal void ratio function for small strain shear modulus. *Fifth International Conference on Recent Advances in Geotechnical Earthquake Engineering and Soil Dynamics, San Diego*.

Carlsten, P. (1988). *Torv – geotekniska egenskaper och byggmetoder*. Linköping: SGI.

Comas X, Slater L & Reeve A. (2004). Geophysical evidence for peat basin morphology and stratigraphic controls on vegetation observed in a northern peatland. *Journal of hydrology*, 295, pp.173-184.

Dahlin, T., Larsson, R., Leroux, V., Svensson, M. & Wisén, R. (2001) *Geofysik i släntstabilitetsutredningar*. Linköping: SGI.

Fox, P.J., Edil, T.B. & Lan, L. Calpha/Cc concept applied to compression of peat. Technical note. (1993). *International Journal of Rock Mechanics and Mining Sciences & Geomechanics Abstracts*, 30(2), p.A85.

Franzén, L.G. & Ljung, T.L. (2009). *A carbon fibre composite (CFC) Byelorussian peat corer*. Gothenburg: Department of Earth Sciences, University of Gothenburg and SU/Ortopedteknik.

Gadallah, M. & Fisher, R. (2009). *Exploration geophysics*. Berlin: Springer.

Google Maps. (2018). *Map data: Google*. Retrieved from https://www.google.com/maps/@58.6410902,11.8013236,10.24z

Hardin, B. O. & Drnevich, V. P. (1972). Shear modulus and damping in soils: Measurement and parameter effects. *Journal of Soil Mechanics & Foundations division*, 98(SM6), pp.603–624.

Hardin, B. O. & Richart, Jr. (1963) Elastic Wave Velocities in Granular Soils. *Journal of the Soil Mechanics and Foundations Division*, 1, pp.33-66.

Hobbs, N.B. (1986). Mire morphology and the properties and behaviour of some British and foreign peats. *Quarterly Journal of Engineering Geology*, 19, 7–80.

Huat, B., Prasad, A., Asadi, A. & Kazemian, S. (2014). *Geotechnics of organic soils and peat*. Boca Raton: CRC Press.

Jowsey, P.C. (1965). *An improved peat sampler*. Aberdeen: The Macaulay Institute for Soil Research.

Korhonen, O. & Lojander, M. (n.d.) *Settlement estimation by using continuous oedometer tests*. Helsinki: Geotechnical Division of the City of Helsinki and University of Technology.

Landstreet, J. (2009, February 9). Planets. Retrieved from Astronomy and Astrophysics: http://www.astro.uwo.ca/~jlandstr/planets/webfigs/earth/images/waves.gif

L'Heureux, J. & Long, M. (2017). Relationship between Shear-Wave Velocity and Geotechnical Parameters for Norwegian Clays. *Journal of Geotechnical and Geoenvironmental Engineering*, 143(6), pp.04017013.

Leroueil, S., Tavenas, F., Samson, L. & Morin, P. (1983). Preconsolidation pressure of Champlain clays. Part II. Laboratory determination. *Canadian Geotechnical Journal*, 20(4), pp.803-816.

Lipiński, M., Wdowska, M. and Jaroń, Ł. (2017). Shear Wave Velocity for Evaluation of State of Cohesionless Soils with Fines. *IOP Conference Series: Materials Science and Engineering*, 245. pp.032083.

Long, M. & Boylan, N. (2012). In Situ Testing of Peat – a Review and Update on Recent Developments. *Geotechnical Engineering Journal of the SEAGS & AGSSEA*, 43(4), pp.41-55.

Long, M., & Boylan, N. (2013). Predictions of settlement in peat soils. *Quarterly Journal of Engineering Geology and Hydrogeology, 46*, 303-322.

Magnusson, O., Sällfors, G. & Larsson, R. (1989). *Ödometerförsök enligt CRS-metoden*. Stockholm: Statens råd för byggnadsforskning.

Mesri, G. & Ajlouni, M. (2007). Engineering Properties of Fibrous Peats. *Journal of Geotechnical and Geoenvironmental Engineering*, 133(7), pp.850-866.

Mesri, G., Stark, T., Ajlouni, M. & Chen, C. (1997). Secondary Compression of Peat with or without Surcharging. *Journal of Geotechnical and Geoenvironmental Engineering*, 123(5), pp.411-421.

Milsom, J. & Eriksen, A. (2011). *Field geophysics*. Hoboken: Wiley.

Mofidpoor, M., Krzic, M. & Principe, L. (2009). Effects of peat source and length of storage time in bales on selected properties of Sphagnum peat. *Canadian Journal of Soil Science*, 89(5), pp.635-644.

Neal, A. (2004). Ground-penetrating radar and its use in sedimentology: principles, problems and progress. *Earth-Science Reviews*, 66(3-4), pp.261-330.

Olsson, M. (2010). *Calculating long-term settlement in soft clays – with special focus on the Gothenburg region*. Linköping: SGI.

Proulx-McInnis, S., St-Hilaire, A., Rousseau, A. & Jutras, S. (2013). A review of ground-penetrating radar studies related to peatland stratigraphy with a case study on the determination of peat thickness in a northern boreal fen in Quebec, Canada. *Progress in Physical Geography*, 37(6), pp.767-786.

Styles, P. (2012). *Environmental Geophysics: Everything you ever wanted (needed!) to know but were too afraid to ask!* Houten: EAGE publ.

Smith, R.E. & Wahls, H.E. (1969). Consolidation Under Constant Rates of Strain. *Journal of the Soil Mechanics and Foundations Division*, 95(2), pp.519-540.

Sällfors, G. (1975). *Preconsolidation pressure of soft, high plastic clay*. Gothenburg: Chalmers University of Technology.

Sällfors, G. (2013). *Geoteknik: Jordmateriallära, jordmekanik*. Göteborg: Cremona.

Sällfors, G. & Andréasson, L. (1986). *Kompressionsegenskaper – Geotekniska laboratorieanvisningar, del 10.* Stockholm: Statens råd för byggnadsforskning.

Trafford, A. (2017). *In Situ Measurement of Shear Wave Velocity and its use in the Determination of Undrained Shear Strength of Peat*. Dublin: University College Dublin.

Trafford, A. & Long, M. (2016) Some recent developments on geophysical testing of peat. *Proceedings 17th Nordic Geotechnical Meeeting (NGM), Reykjavik*, pp.215 – 224

Vesterberg, B., Carlsten, P. & Lindh, P. (2016). *Erfarenheter av byggmetoder på torvmark.* Linköping: SGI.

Von Post, L. & Granlund, E. (1926). Peat resources in southern Sweden. *Sveriges Geologiska Undersökning, Yearbook*, 335, pp.1–127.

Yong, R.N. & Townsend, F.C. (1986). *Consolidation of soils: testing and evaluation*. Philadelphia: American Society for Testing and Materials.

Yulindasari, S. (2006) *Compressibility characteristics of fibrous peat soil*. Masters Dissertation. Universiti Teknologi Malaysia.

Appendix

The plots of effective stress against strain generated from the 13 CRS-tests are shown below.

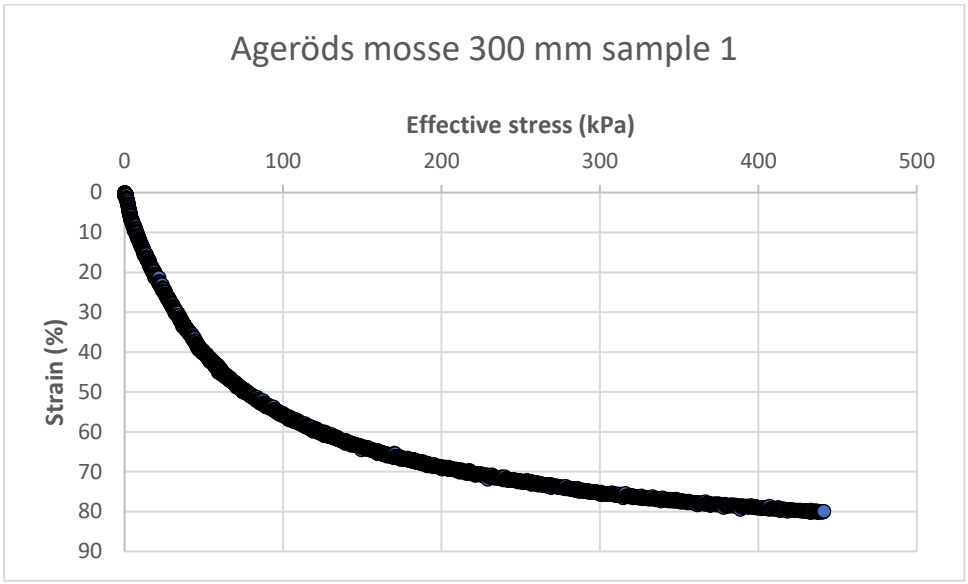

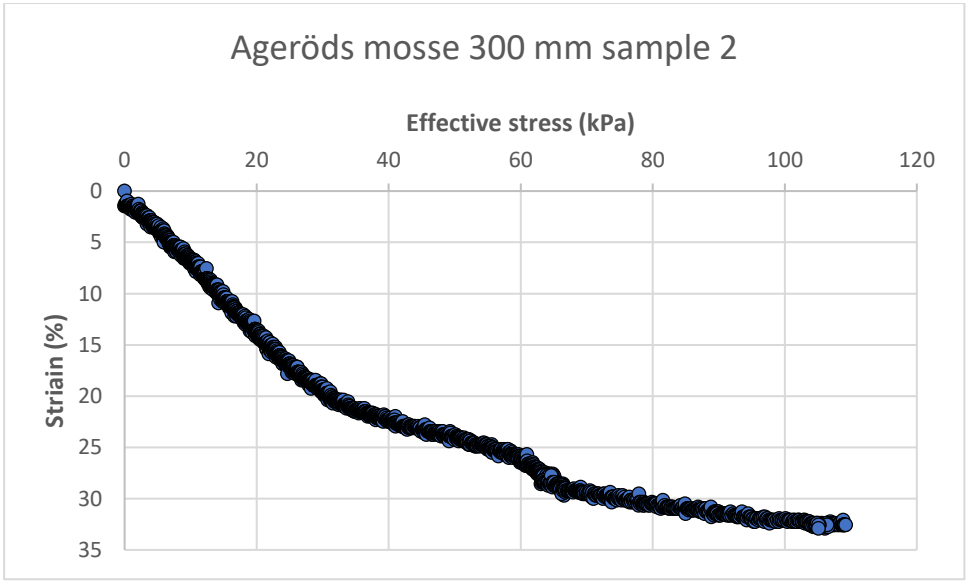

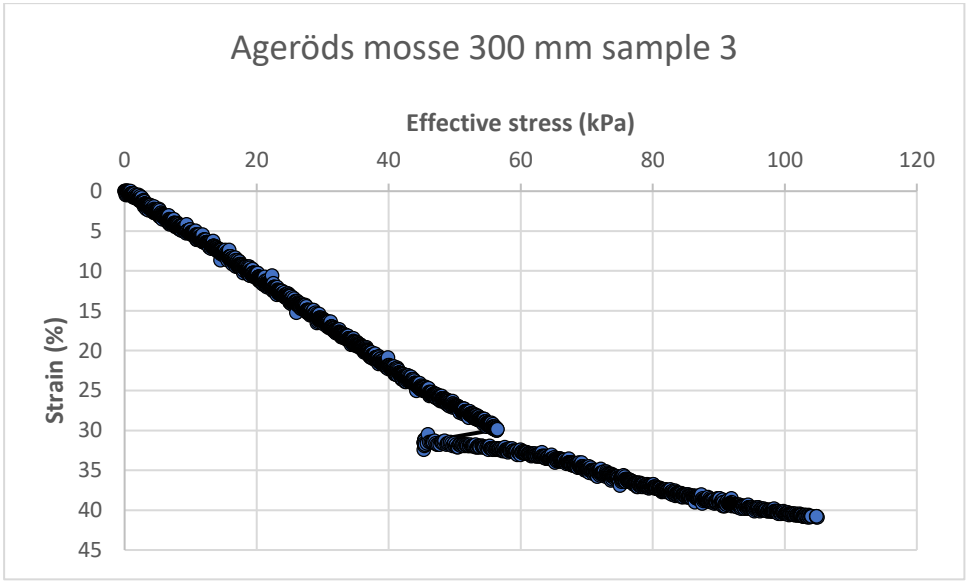
Ageröds mosse 300 mm sample 3
Effective stress (kPa)
0
20
40
60
80
100
120
Strain (%)
0
5
10
15
20
25
30
35
40
45

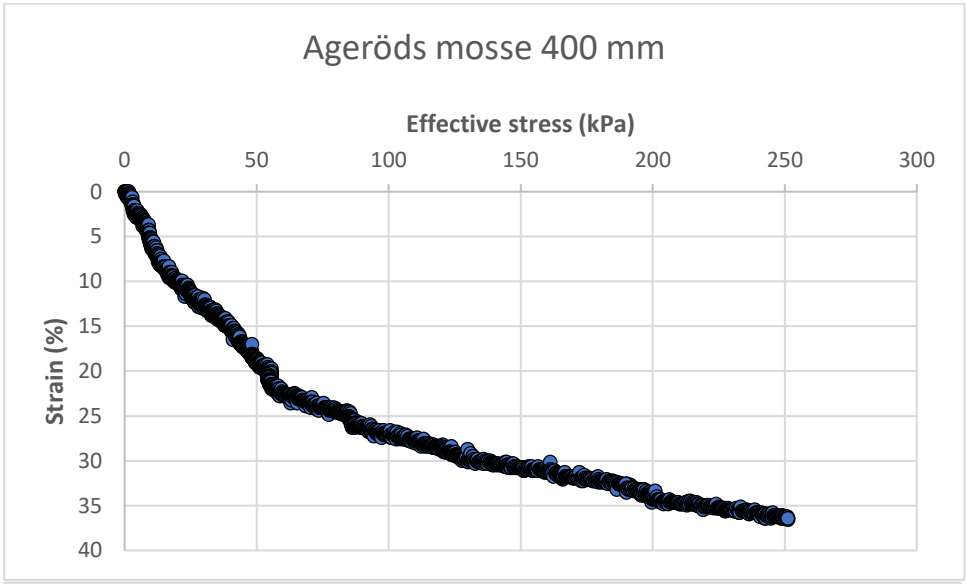
Ageröds mosse 400 mm
Effective stress (kPa)
0
50
100
150
200
250
300
Strain (%)
0
5
10
15
20
25
30
35
40

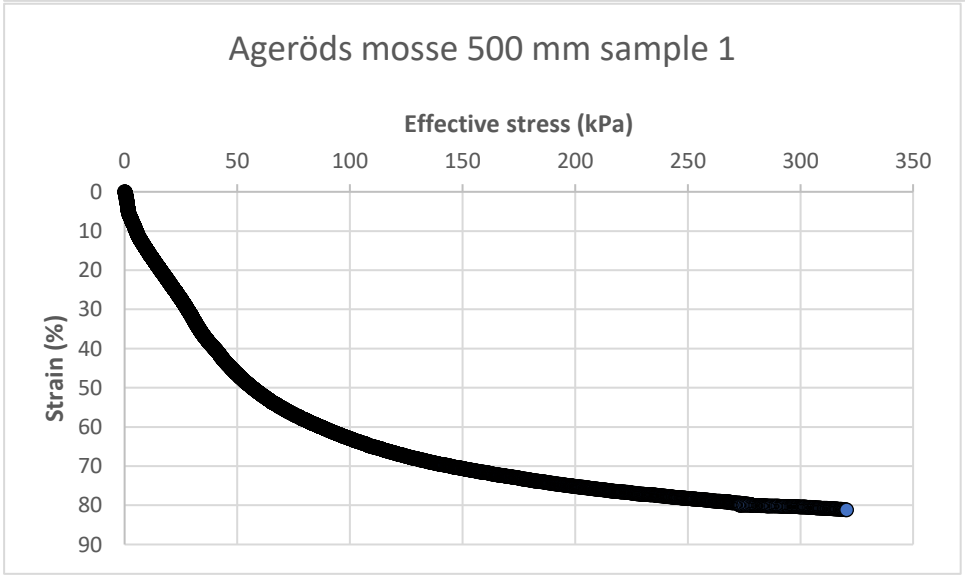
Ageröds mosse 500 mm sample 1
Effective stress (kPa)
0
50
100
150
200
250
300
350
Strain (%)
0
10
20
30
40
50
60
70
80
90

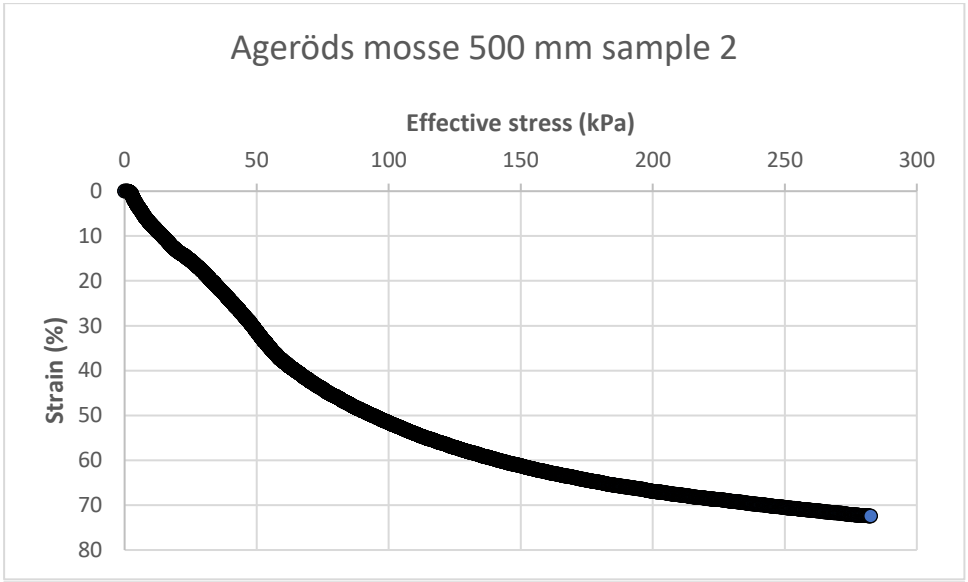
Ageröds mosse 500 mm sample 2
Effective stress (kPa)
0
50
100
150
200
250
300
Strain (%)
0
10
20
30
40
50
60
70
80

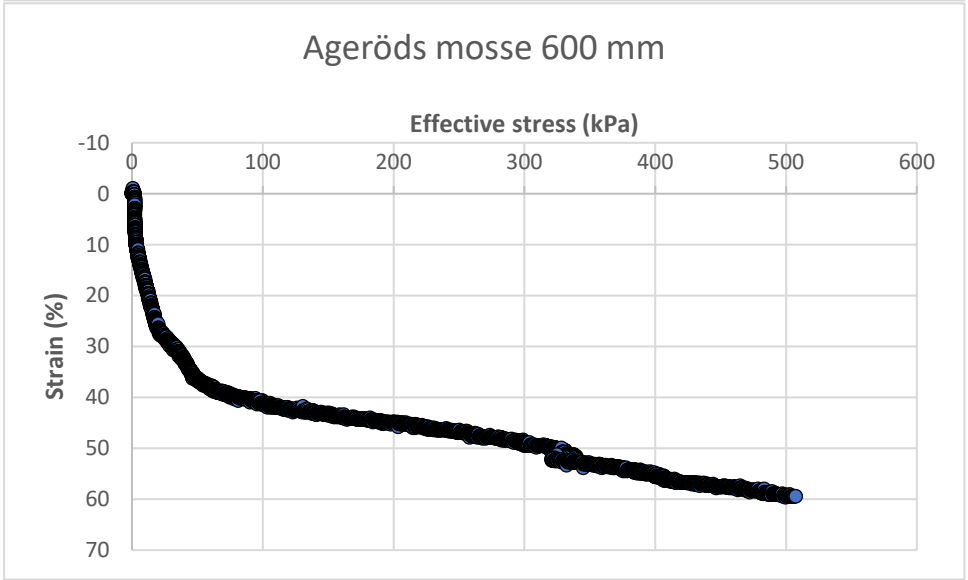
Ageröds mosse 600 mm
Effective stress (kPa)
-10
0
100
200
300
400
500
600
Strain (%)
0
10
20
30
40
50
60
70

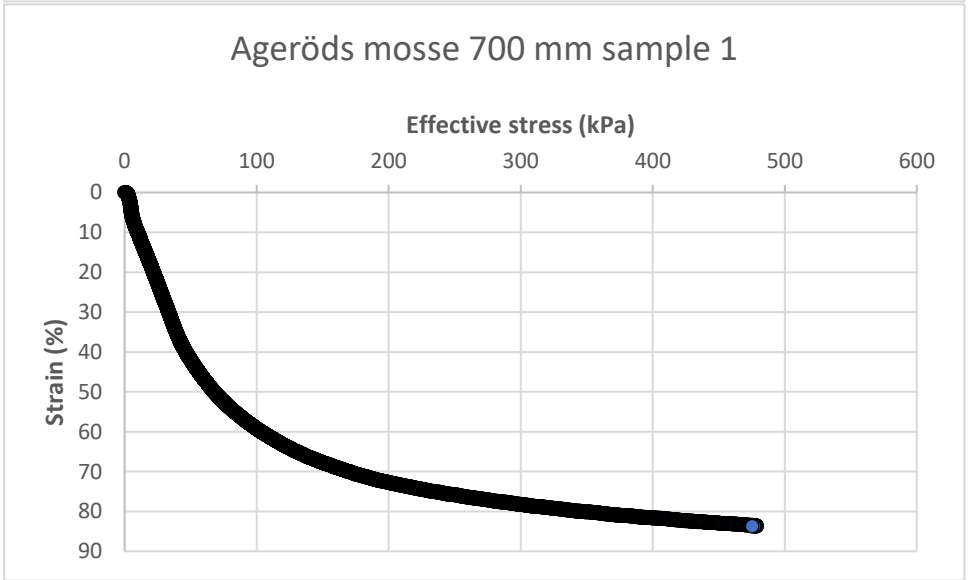
Ageröds mosse 700 mm sample 1
Effective stress (kPa)
0
100
200
300
400
500
600
Strain (%)
0
10
20
30
40
50
60
70
80
90

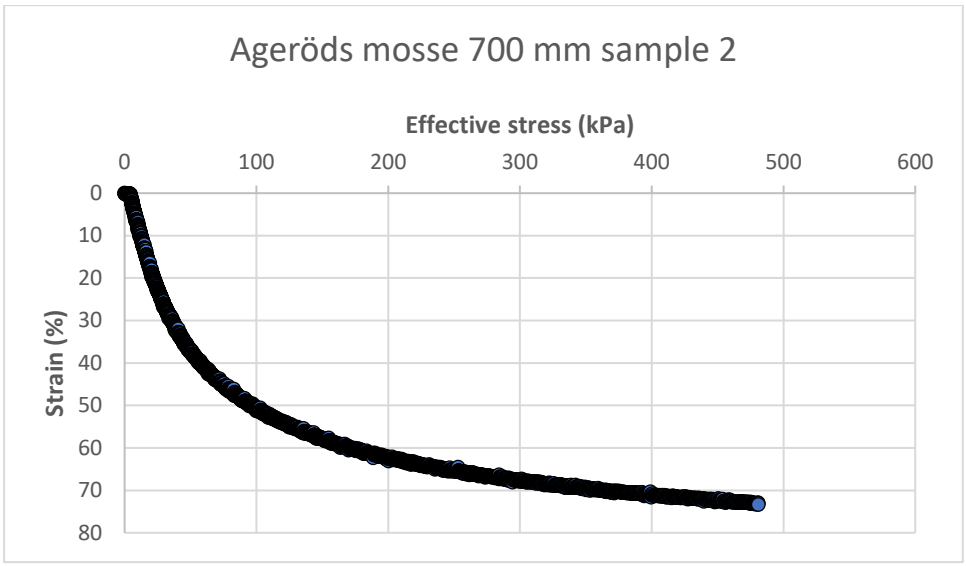
Ageröds mosse 700 mm sample 2
Effective stress (kPa)
0
100
200
300
400
500
600
Strain (%)
0
10
20
30
40
50
60
70
80

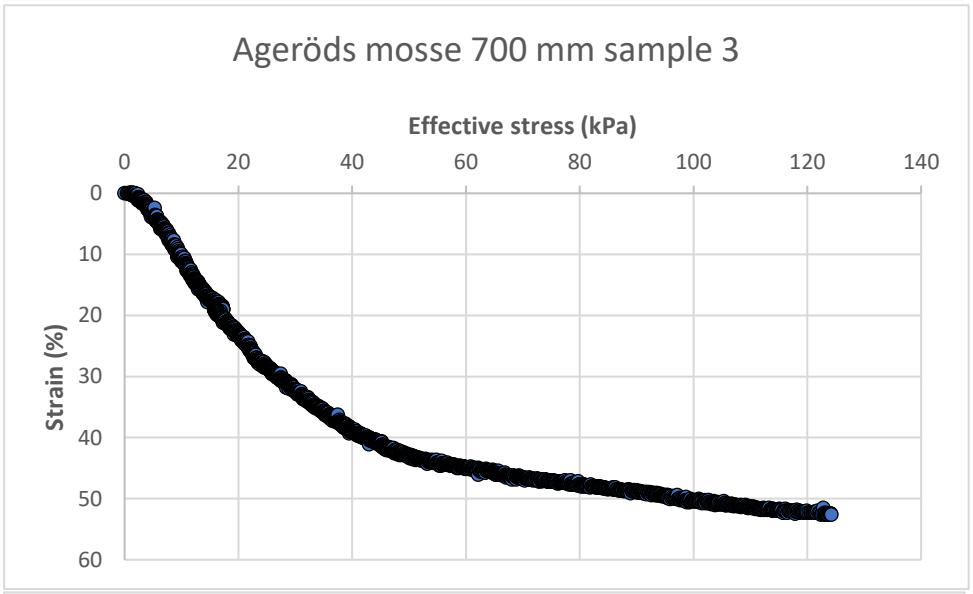
Ageröds mosse 700 mm sample 3
Effective stress (kPa)
0
20
40
60
80
100
120
140
Strain (%)
0
10
20
30
40
50
60

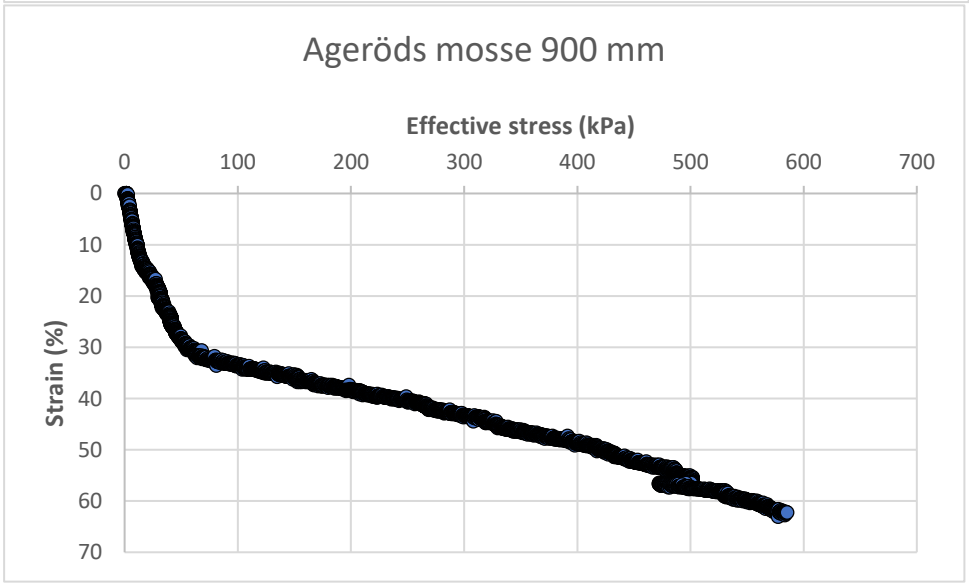
Ageröds mosse 900 mm
Effective stress (kPa)
0
100
200
300
400
500
600
700
Strain (%)
0
10
20
30
40
50
60
70

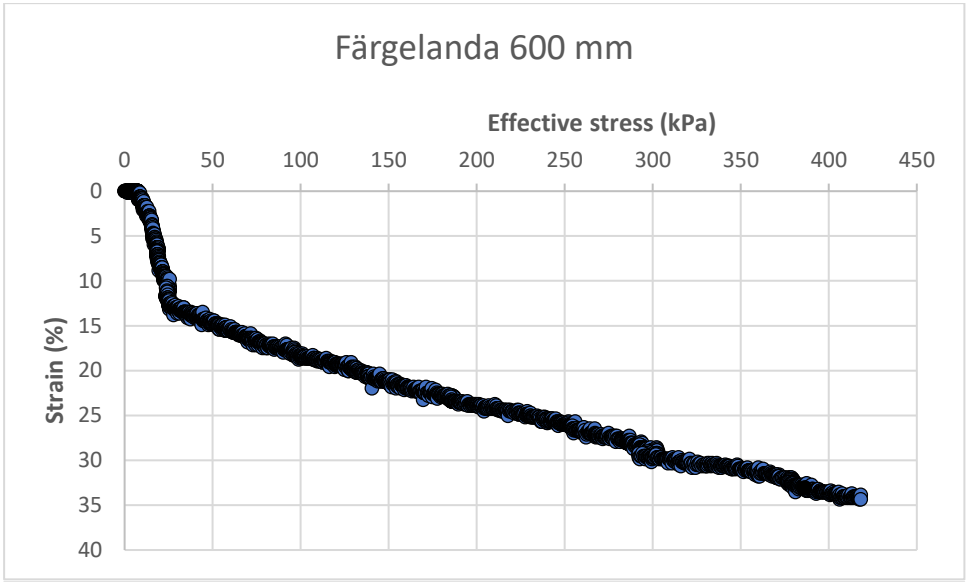
Färgelanda 600 mm
Effective stress (kPa)
0
50
100
150
200
250
300
350
400
450
Strain (%)
0
5
10
15
20
25
30
35
40

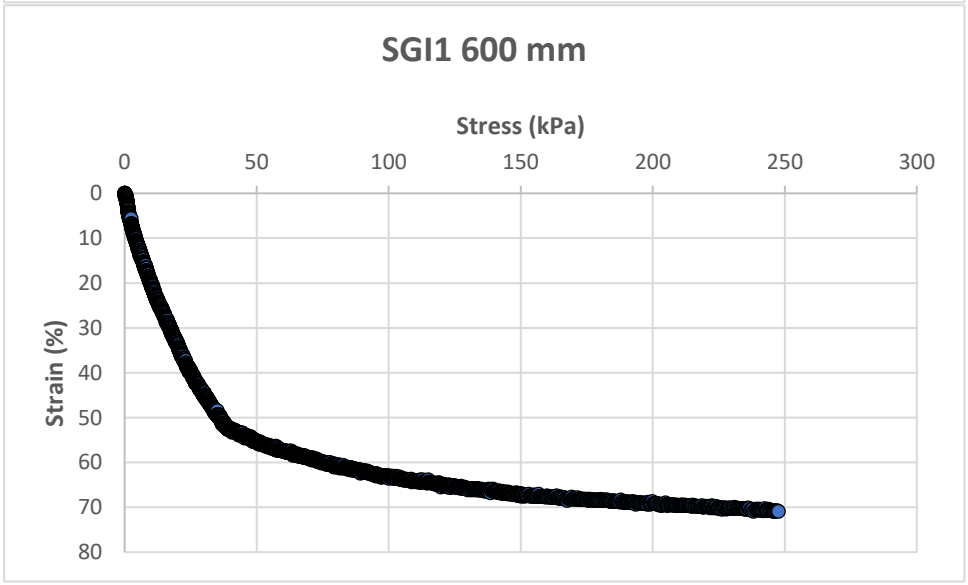
SGI1 600 mm
Stress (kPa)
0
50
100
150
200
250
300
Strain (%)
0
10
20
30
40
50
60
70
80